

In presenting the dissertation as a partial fulfillment of the requirements for an advanced degree from the Georgia Institute of Technology, I agree that the Library of the Institution shall make it available for inspection and circulation in accordance with its regulations governing materials of this type. I agree that permission to copy from, or to publish from, this dissertation may be granted by the professor under whose direction it was written, or, in his absence, by the Dean of the Graduate Division when such copying or publication is solely for scholarly purposes and does not involve potential financial gain. It is understood that any copying from, or publication of, this dissertation which involves potential financial gain will not be allowed without written permission.

MINIMIZATION OF CREEP-TIME EFFECTS IN PHOTOELASTIC
INVESTIGATIONS

A THESIS

Presented to
the Faculty of the Graduate Division
Georgia Institute of Technology

In Partial Fulfillment
of the Requirements for the Degree
Master of Science in Mechanical Engineering


by
Charles Howard Parr

April 1956

8¹²
12^T

MINIMIZATION OF CREEP-TIME EFFECTS IN PHOTOELASTIC
INVESTIGATIONS

Approved:



Date Approved by Chairman: May 21, 1956

ACKNOWLEDGEMENTS

At the completion of this work, I would like to express my sincere thanks to Dr. Joseph P. Vidosic, my advisor, for the suggestion of the problem and guidance during the study. My thanks also to J. D. Clem, Jr., who helped materially during the latter portion of the laboratory work.

TABLE OF CONTENTS

	Page
ACKNOWLEDGEMENTS	ii
LIST OF TABLES	iv
LIST OF ILLUSTRATIONS	v
SUMMARY	vii
CHAPTER	
I. INTRODUCTION TO THE PROBLEM	1
II. THEORETICAL ANALYSIS	5
III. EQUIPMENT AND MODELS	10
IV. EXPERIMENTAL PROCEDURE	19
V. DISCUSSION OF RESULTS	25
VI. CONCLUSIONS	28
VII. RECOMMENDATIONS	30
APPENDIX	31
BIBLIOGRAPHY	62

LIST OF TABLES

TABLE		Page
1.	Optical Creep of Beam in Pure Bending, Constant Load	47
2.	Optical Creep of Beam in Pure Bending, Constant Strain	48
3.	Optical Creep of Beam in Pure Bending, Dynamometer Load	49
4.	Optical Creep of Beam, Concentrated Load, Dynamometer Load	50
5.	Optical Creep of Beam, Concentrated Load, Constant Strain	51
6.	Optical Creep of Beam, Concentrated Load, Constant Load	52
7.	Optical Creep of Tensile Bar, Constant Load	53
8.	Optical Creep of Tensile Bar, Dynamometer Load. .	54
9.	Optical Creep of Tensile Bar, Constant Strain. . . .	55
10.	Optical Creep of Curved Beam, Constant Strain . . .	56
11.	Optical Creep of Curved Beam, Dynamometer Load	57
12.	Optical Creep of Curved Beam, Constant Load. . . .	58
13.	Optical Creep of Disk in Compression, Constant Load.	59
14.	Optical Creep of Disk in Compression, Dynamometer Load	60
15.	Optical Creep of Disk in Compression, Constant Strain.	61

LIST OF ILLUSTRATIONS

FIGURE		Page
1.	Dynamometer Loading Fixture	2
2.	Creep Balance Mechanism.	4
3.	Schematic Diagram of Polariscope	11
4.	Polariscope in Stress Analysis Laboratory	12
5.	Loading Frame and Method of Loading.	13
6.	Beam Fabrication Jig.	15
7.	a. Specimen Type "A"	16
	b. Specimen Type "B"	16
	c. Specimen Type "C"	17
	d. Specimen Type "D"	17
	e. Specimen Type "E"	17
8.	Constant Load Device	20
9.	Constant Strain Device	21
10.	Dynamometer Loading Device	22
11.	Optical Creep of Beam in Pure Bending, Constant Load	32
12.	Optical Creep of Beam in Pure Bending, Constant Strain.	33
13.	Optical Creep of Beam in Pure Bending, Dynamometer Load.	34
14.	Optical Creep of Beam, Concentrated Load, Dynamometer Load	35
15.	Optical Creep of Beam, Concentrated Load, Constant Strain	36

FIGURE

16.	Optical Creep of Beam, Concentrated Load, Constant Load	37
17.	Optical Creep of Tensile Bar, Constant Load	38
18.	Optical Creep of Tensile Bar, Dynamometer Load. .	39
19.	Optical Creep of Tensile Bar, Constant Strain. . . .	40
20.	Optical Creep of Curved Beam, Constant Strain. . .	41
21.	Optical Creep of Curved Beam, Dynamometer Load.	42
22.	Optical Creep of Curved Beam, Constant Load. . . .	43
23.	Optical Creep of Disk in Compression, Constant Load.	44
24.	Optical Creep of Disk in Compression, Dynamometer Load	45
25.	Optical Creep of Disk in Compression, Constant Strain.	46

SUMMARY

Two loading mechanisms were investigated to determine their practicability for minimizing creep-time effects in photoelastic materials. The two mechanisms were: (1) a device to apply a constant strain to the photoelastic model, and (2) a device to apply a load to the model through a spring loaded dynamometer. Limited work had previously shown that both mechanisms, when compared with the commonly used constant load method of stressing a model, reduced the creep-time effect.

A theoretical analysis shows that the results to be expected with each device are dependent on both the photoelastic material and model geometry. Experimental tests were made with only one photoelastic material, CR-39, which has a relatively large creep-time effect under a constant load. Five model types were tested. Both devices were found to reduce creep markedly for some model shapes. Over a two hour period, total creep as low as one per cent of the fringe order was measured with both devices. The creep rate was found to vary with the model shape and the method of loading. Although the two devices are comparable in minimization of creep-time effects in CR-39, the spring loaded dynamometer is preferred because of its simplicity of operation.

Further investigation of the two devices using other photoelastic materials is suggested by the results. The effects of stress

concentrations near loading points of the model on creep effects may also be worthy of investigation.

CHAPTER I

INTRODUCTION TO THE PROBLEM

In photoelastic investigations it is often necessary for the measurement of isochromatics and isoclinics to extend over a considerable period of time while the model is in a stressed condition. However, many photoelastic materials, when stressed, exhibit a high rate of optical creep, i. e., a rapid change of the fringe pattern with time. This, obviously, is undesirable since there may be a considerable difference in the fringe pattern exhibited by the model over a period of time, thus leading to innate errors in observation of fringe values.

It would be desirable, then, to have a method of maintaining a constant fringe pattern throughout an experiment or to have a method of obtaining corrections for the changing fringe pattern. It was the purpose of this investigation to determine the practicability of two proposed loading devices to obtain these ends. The commonly used constant load device was to be replaced with one of the following devices.

(1) A spring loaded dynamometer scale to apply the load. It was believed that the dynamometer would partially release the load as the strain in the model increased with time, thus decreasing the stress and to some extent compensating for the optical creep in the model. A schematic diagram of this apparatus is shown in Figure 1.

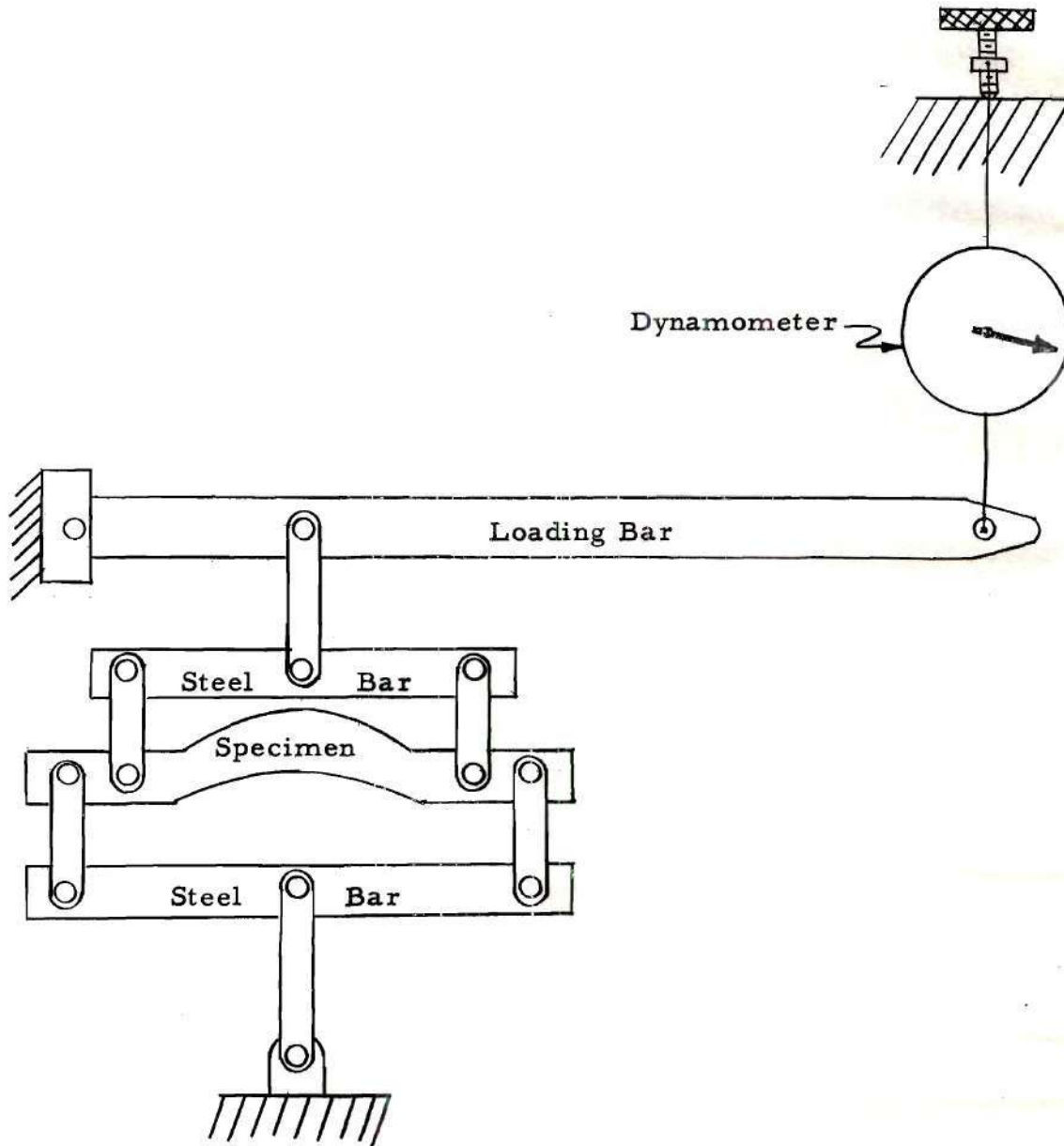


Figure 1

Dynamometer Loading Fixture

(2) A creep balance which would apply a fixed deflection to the model, thus eliminating optical creep if the optical creep was proportional only to physical creep. A further extension of this method would allow a calibration model to be placed in series with the test model so that instantaneous values of the fringe coefficient could be found as the test progresses. A diagram of the creep balance is shown in Figure 2.

Previous work with the two methods consisted of a small amount of unpublished data by Dr. J. P. Vidosic¹. This data was preliminary and inconclusive. Investigation of creep properties of photoelastic materials has been done by Filon and Coker (1), et al. A discussion of various empirical equations for creep in celluloid, bakelite and India rubber is given in reference (1).

The creep balance was proposed by Charles H. Norris (2) and has been used at the Massachusetts Institute of Technology. This work, using Bakelite BT-48-306 as a photoelastic material, indicated that the creep balance was capable of eliminating optical creep.

¹Professor of Mechanical Engineering, Georgia Institute of Technology.

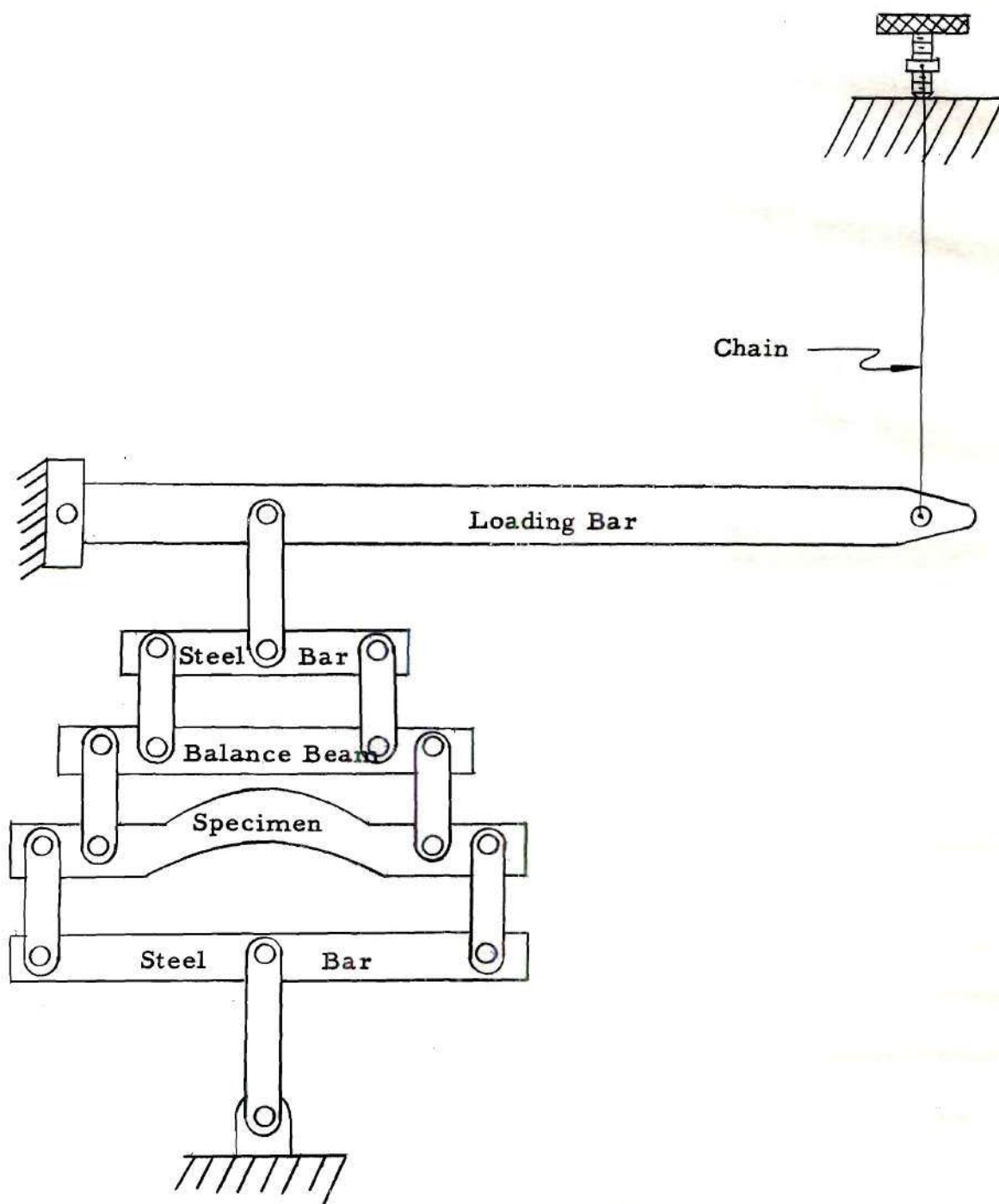


Figure 2
Creep Balance Mechanism

CHAPTER II

THEORETICAL ANALYSIS

In the work of Filon and Coker (1) it has been shown that the optical effect may be proportional to either stress or strain, or stress and strain, depending on the photoelastic material used. Clearly this fact is of secondary importance while working with a perfectly elastic material but in the plastic region or while working with creep effects it is of paramount importance. Let us assume a material whose optical retardation is proportional to both stress and strain and is of the form:

$$r = \alpha \sigma + \beta \epsilon \quad (1)$$

where

- r = retardation,
- α, β = constants of the material,
- σ = stress,
- ϵ = strain.

In the proportional region of this material

$$\epsilon = \frac{\sigma}{E}, \quad (2)$$

where

- E = modulus of elasticity,

and equation (1) may be written

$$r = \left(\alpha + \frac{\beta}{E} \right) \sigma, \quad (3)$$

or

$$r = (\alpha E + \beta) \epsilon, \quad (4)$$

if it is assumed that there are no creep effects.

If this material is now observed over a period of time while loaded in a constant load device, the optical pattern will change as the strain continually increases and the stress remains essentially constant. However, since creep can be thought of as a change in the modulus of elasticity of a material with time, a material may creep while maintaining a constant deflection, by reducing the stress of the material¹. This would indicate that a constant strain device would not eliminate optical creep in a material whose retardation is proportional to both stress and strain—a "two parameter" material. The optical creep would be eliminated only if the stress constant, " α ", for the particular material was zero.

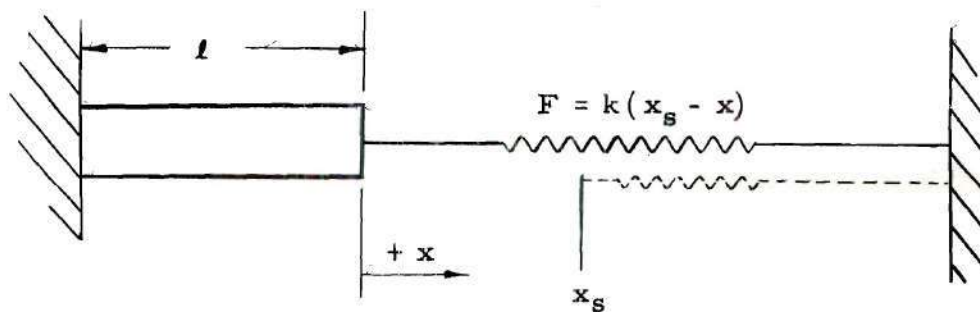
This analysis has shown that for a "two parameter" material, neither a constant load nor a constant strain loading device will eliminate optical creep if the modulus of elasticity of the material changes with time. The amount of minimization obtained with each device will depend on the properties of the individual material.

The dynamometer scale method of loading is intermediate between the constant load and constant strain devices. The mechanism

¹The concept of a changing modulus is more fully discussed in terms of a "relaxed elastic modulus" in reference (3), pp 41 - 47.

is such that a creep in the model will cause a slight decrease in load, which will in turn reduce the tendency for the model to creep. While the actual stress is somewhat reduced in a manner similar to the constant strain device, the model continues its physical creep, not unlike the constant load mechanism.

We may illustrate this action with the following example of a tensile specimen where:



- l = specimen length,
- F = force on specimen,
- A = cross sectional area,
- x_o = initial position of the free end before applying load,
- k = dynamometer spring constant,
- x_s = position at which spring force is zero, i. e., spring in unstressed position.

Generally,

$$\sigma = \frac{F}{A} \quad \text{and} \quad \epsilon = \frac{x}{l} ,$$

but

$$(x_s - x) = \frac{F}{k} ,$$

or

$$x = x_s - \frac{F}{k}.$$

At time t_1 ,

$$\epsilon_1 = \frac{x_1}{l} = \frac{x_s - \frac{F_1}{k}}{l},$$

and

$$\sigma_1 = \frac{F_1}{A}.$$

If

$$r = \alpha \sigma + \beta \epsilon$$

for the material, then

$$r_1 = \frac{\alpha F_1}{A} + \beta \left(\frac{x_s}{l} - \frac{F_1}{k l} \right),$$

which can be written

$$r_1 = \frac{\beta x_s}{l} + F_1 \left(\frac{\alpha}{A} - \frac{\beta}{k l} \right).$$

Since the change in A is very small, the retardation is equal to a constant plus a linear function of F . Thus as long as physical creep occurs there will be a corresponding change in the retardation. Also, it can be seen that the change in retardation is dependent on the geometry of the model as well as the properties of the model material.

The dynamometer scale method of loading would not be capable, then, of eliminating optical creep in a photoelastic material. However, the optical creep may be greatly reduced, depending on the properties of the material used.

CHAPTER III

EQUIPMENT AND MODELS

The polariscope used in this investigation is located in the Stress Analysis Laboratory of the Georgia Institute of Technology. This polariscope is a lens type utilizing Polaroid as the polarizing medium. A schematic diagram of the polariscope is shown in Figure 3 and a picture is shown in Figure 4. A sodium vapor lamp utilizing a filter to give monochromatic light of wave length 5461 \AA was used as a light source. Fringe readings were taken directly from a screen upon which the image was projected. The loading frame for the polariscope was a commonly used type, with a loading bar, hinged on one side of the frame, moving in a vertical plane. The loading force was applied at the opposite end of the bar as shown in Figure 5. The model loading attachment was located so that a four to one magnification of the force applied to the bar was obtained in the model.

Equipment to produce the models included a jigsaw, a drill press, and a Gorton router. The jigsaw was used for cutting the models from the plastic sheet and the final machining was done with the router. This equipment was already available in the laboratory.

Five types of models were used in the investigation. Existing jigs and templates were used since each model was a type previously used in the laboratory. These fixtures included the following:

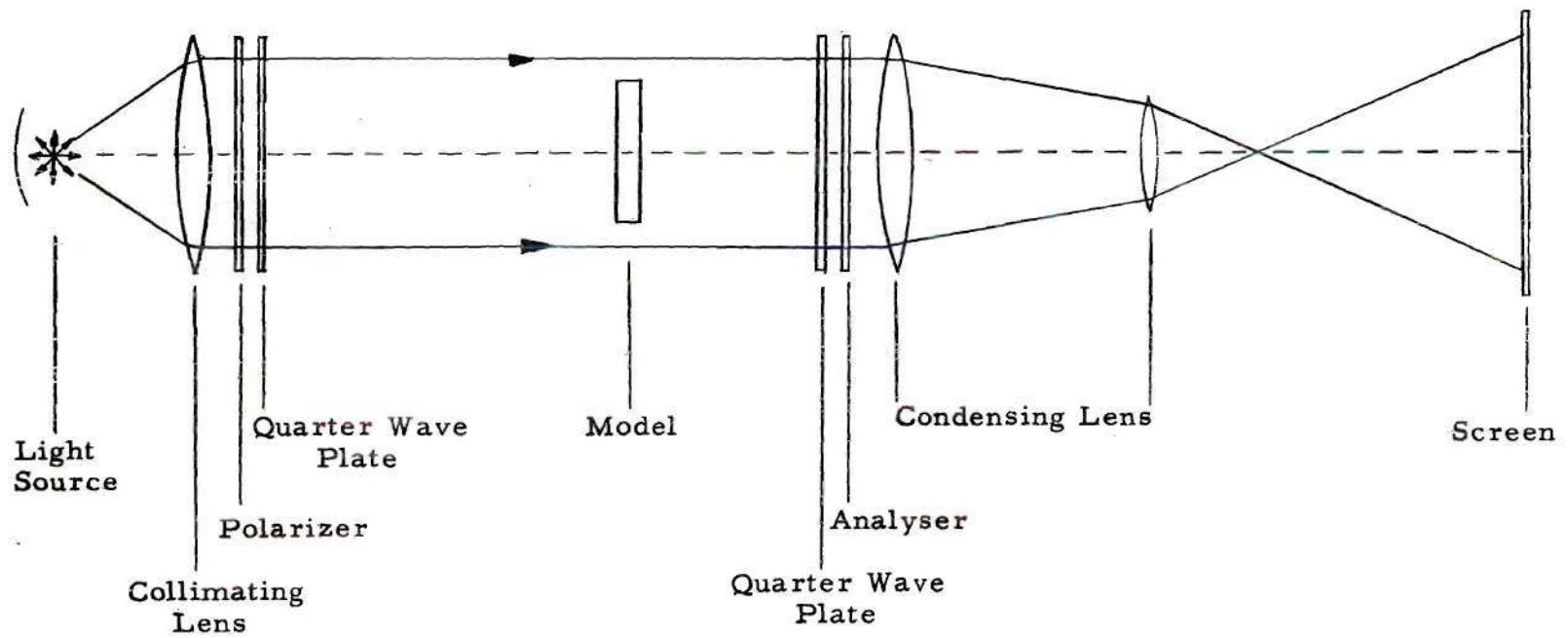


Figure 3
Schematic Diagram of Polariscope

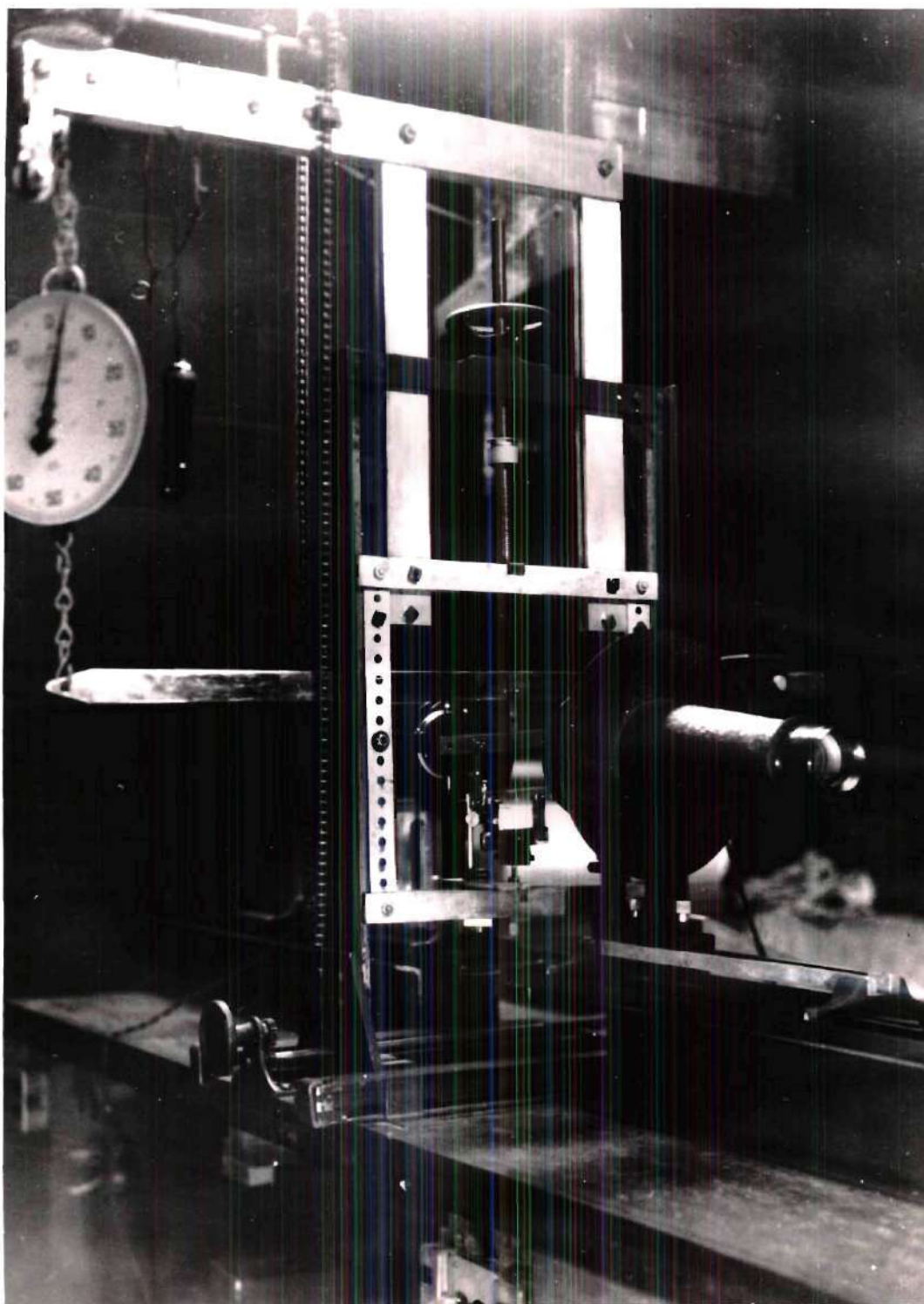


Figure 4

Lens Type Polariscopes with Dynamometer Loading Fixture

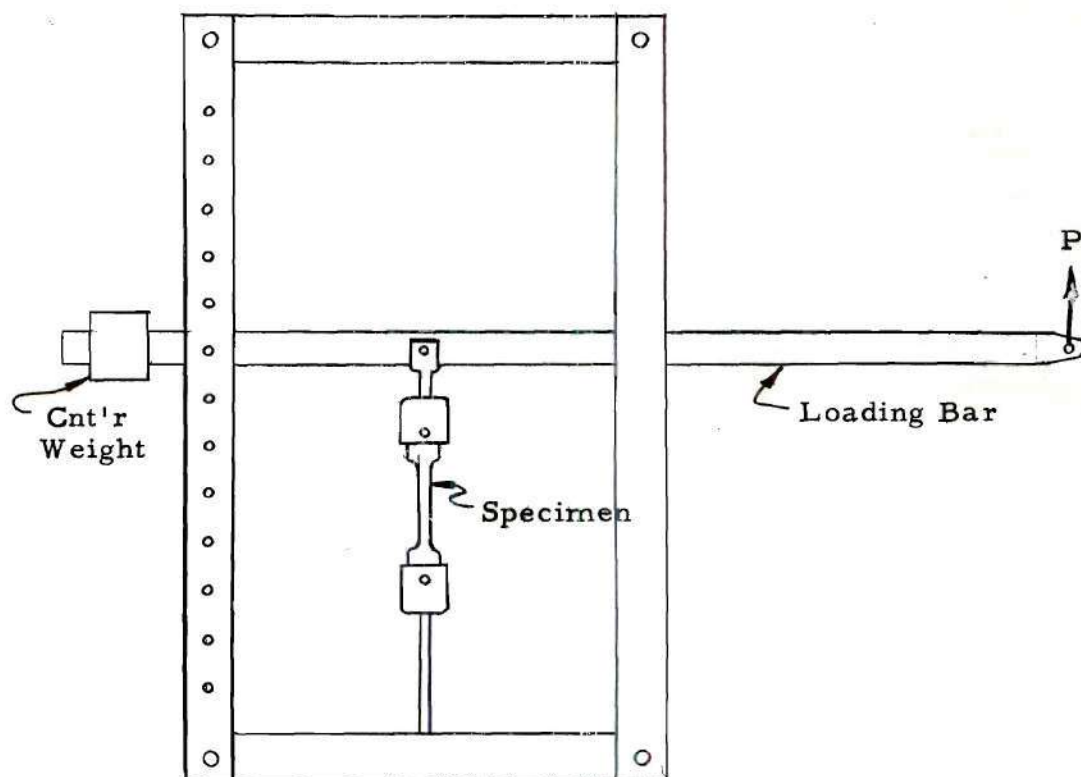


Figure 5
Loading Frame and Method of Loading

- (1) a drill jig for spacing holes on integral inch centers,
- (2) a jig used in conjunction with the router for finish machining the straight beam models (see Figure 6) ,
- (3) a template for finish machining the curved beam models,
- (4) a template for drilling and finish machining the tension models,
- (5) a jig for finish machining the disk models.

Sketches of the models used are shown in Figure 7. The fabrication of all the models was generally similar but each type differed greatly in detail. An outline of the desired specimen was first scribed on a sheet of one-quarter inch thick CR-39 plastic. This is an allyl resin manufactured by the Homalite Corporation¹. The specimen was then cut out with the jigsaw, leaving about one-eighth of an inch between the cut and the scribed line. The jigsaw cut was very jagged and left severe residual stresses in the model near the edges, which were removed in a later operation.

Drilling the required holes was done with ordinary twist drills set aside in the laboratory for this use. Drill feed was by hand and a coolant composed of water and linseed oil was used. Despite the use of the coolant and a very slow drill feed, machining stresses on the order of one fringe were produced around the holes. Reaming did not completely relieve these stresses, but their effect was negligible at the points where measurements of fringe order were taken because of the relatively large distance between the drilled holes and measurement points.

¹11 - 13 Brookside Drive, Wilmington, Delaware.

Back-up Plate

Model

Spacer

Template

Base

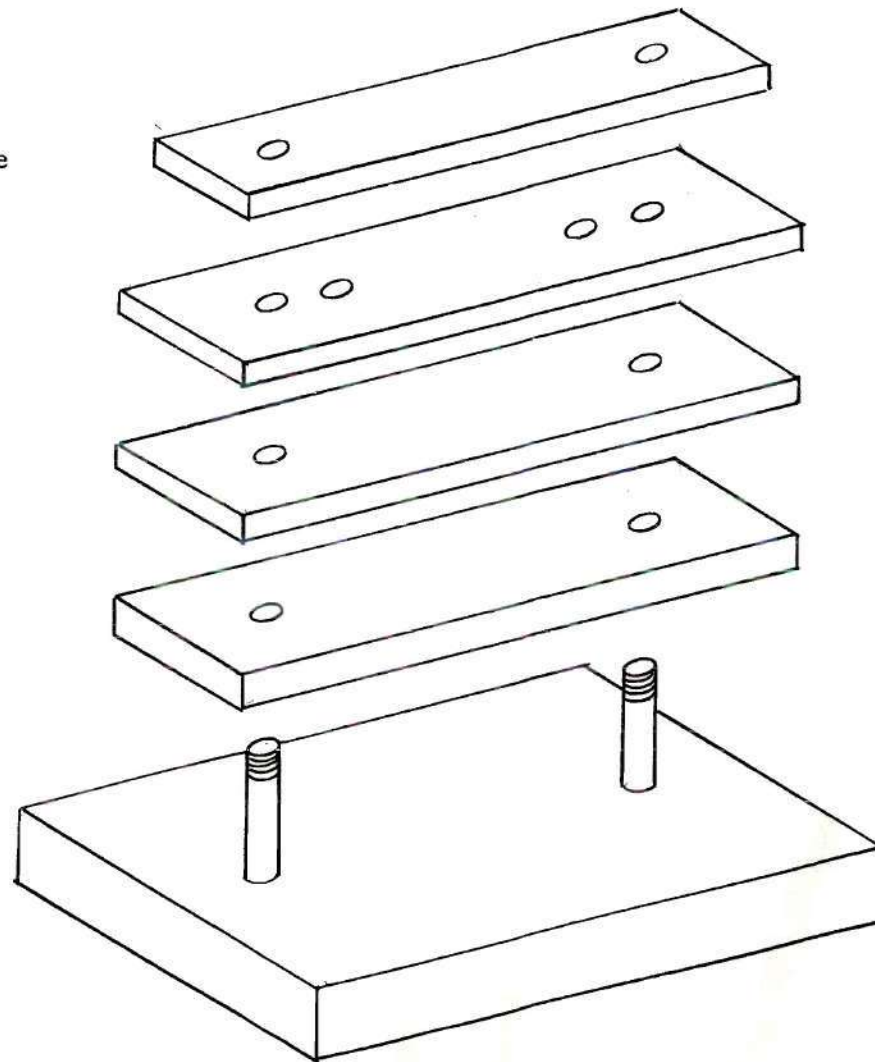
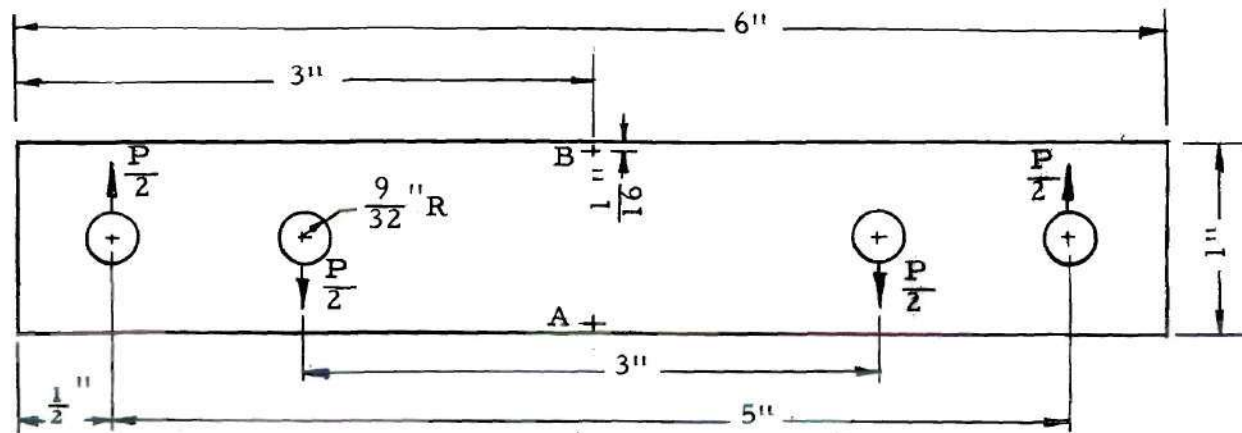
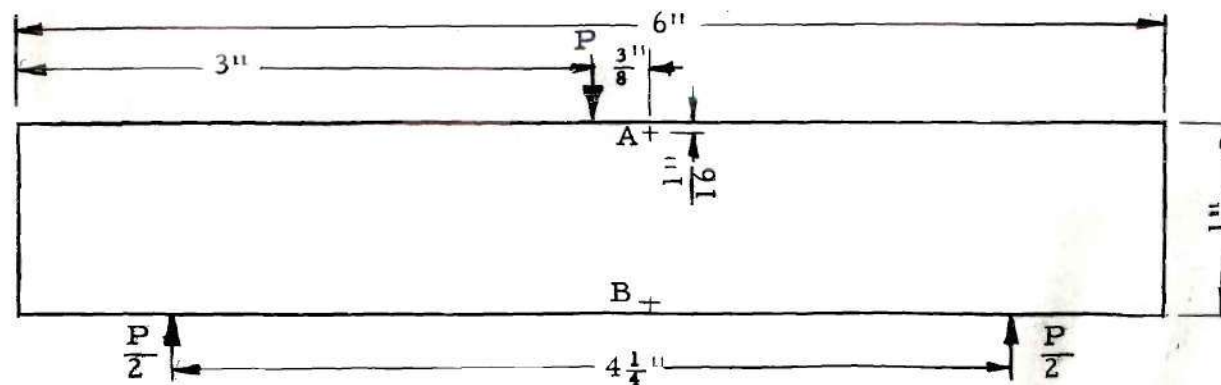


Figure 6
Beam Fabrication Jig



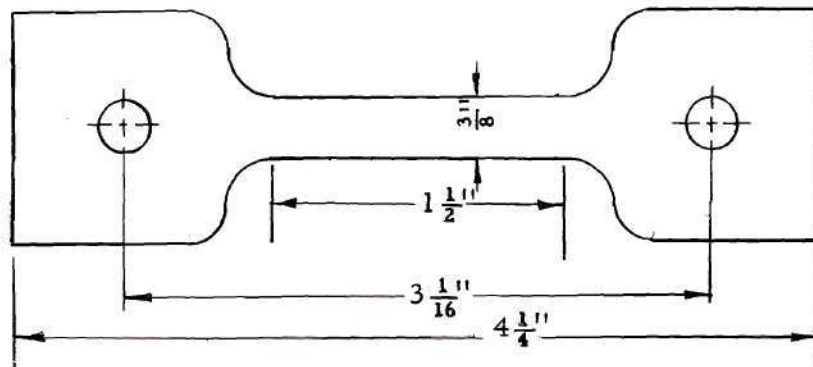
Specimen Type "A"
Beam - Pure Bending

Figure 7 (a)

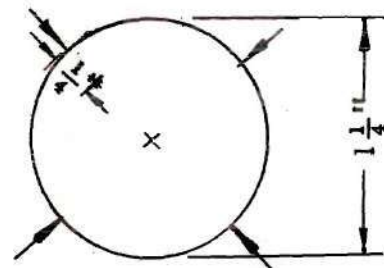


Specimen Type "B"
Beam - Concentrated Load

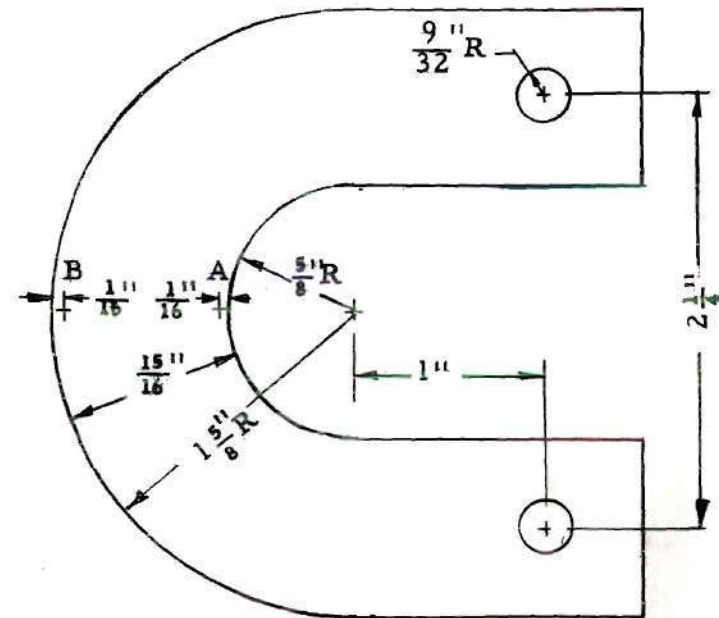
Figure 7 (b)



Specimen Type "C"
Tension
Figure 7 (c)



Specimen Type "E"
Compression Disk
Figure 7 (e)



Specimen Type "D"
Curved Beam
Figure 7 (d)

The final machining operation was done on the router. A circular guide about one inch in diameter was clamped to the table of the router and used as a guide for the jigs. By utilizing the cross feed and varying the position of the guide relative to the cutter, cuts of varying depth could be made. Initial cuts were on the order of 0.015 inches while the finish cut was about 0.002 or 0.003 inch. For the final cut the center of the circular tip of the guide was directly under the center of the cutter. This permitted the jig to be manipulated by hand and rather severe angular deviations in the direction of feed to be made while maintaining a smooth finish cut.

CHAPTER IV

EXPERIMENTAL PROCEDURE

It was desired to investigate the reaction of several types of specimens under three different types of loading. Although the properties of the photoelastic material used might have a great effect on results, it was necessary to limit the investigation to one material, CR-39. This plastic was chosen because it is inexpensive, commonly used, and is generally satisfactory for two-dimensional photoelastic work.

Five specimen types were selected: a beam in pure bending, a beam with concentrated load, a concentric curved beam, a tensile bar, and a disk radially loaded in compression. These types would cover, respectively, the following stress fields: compression and tension due to bending, compression and tension with shear due to bending, compression and tension due to bending with super-imposed tension, simple tension, and compression with shear. Readings were taken at points shown in Figure 7.

The mechanisms used for applying the three types of loading are shown in Figures 8, 9, and 10. To keep the number of variables at a minimum the loading mechanism of each of the three systems was identical with the exception of the way the force was applied to the main loading bar. The constant load was applied by hanging metal weights on a wire fastened to the loading bar and traveling over a

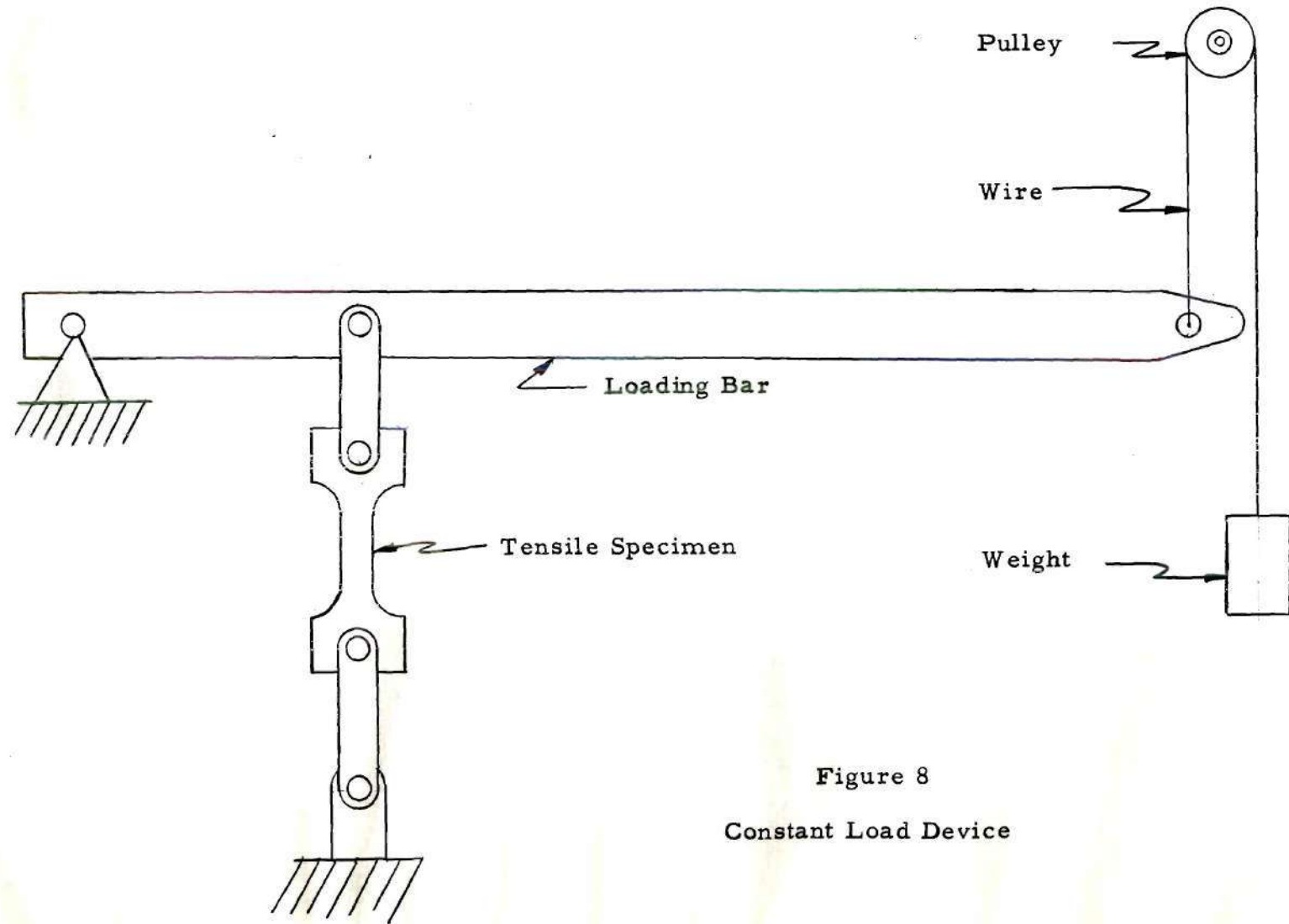


Figure 8
Constant Load Device

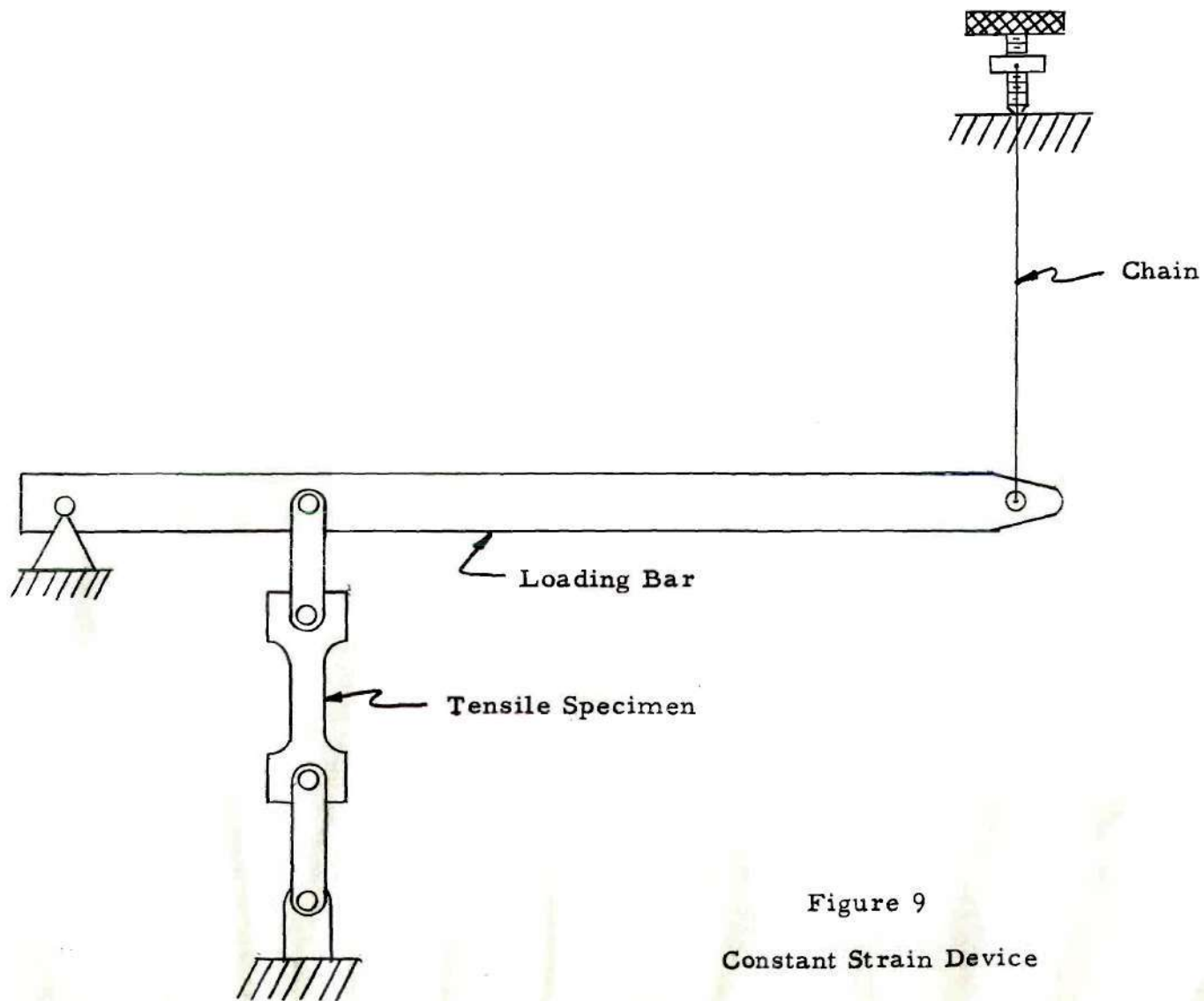


Figure 9
Constant Strain Device

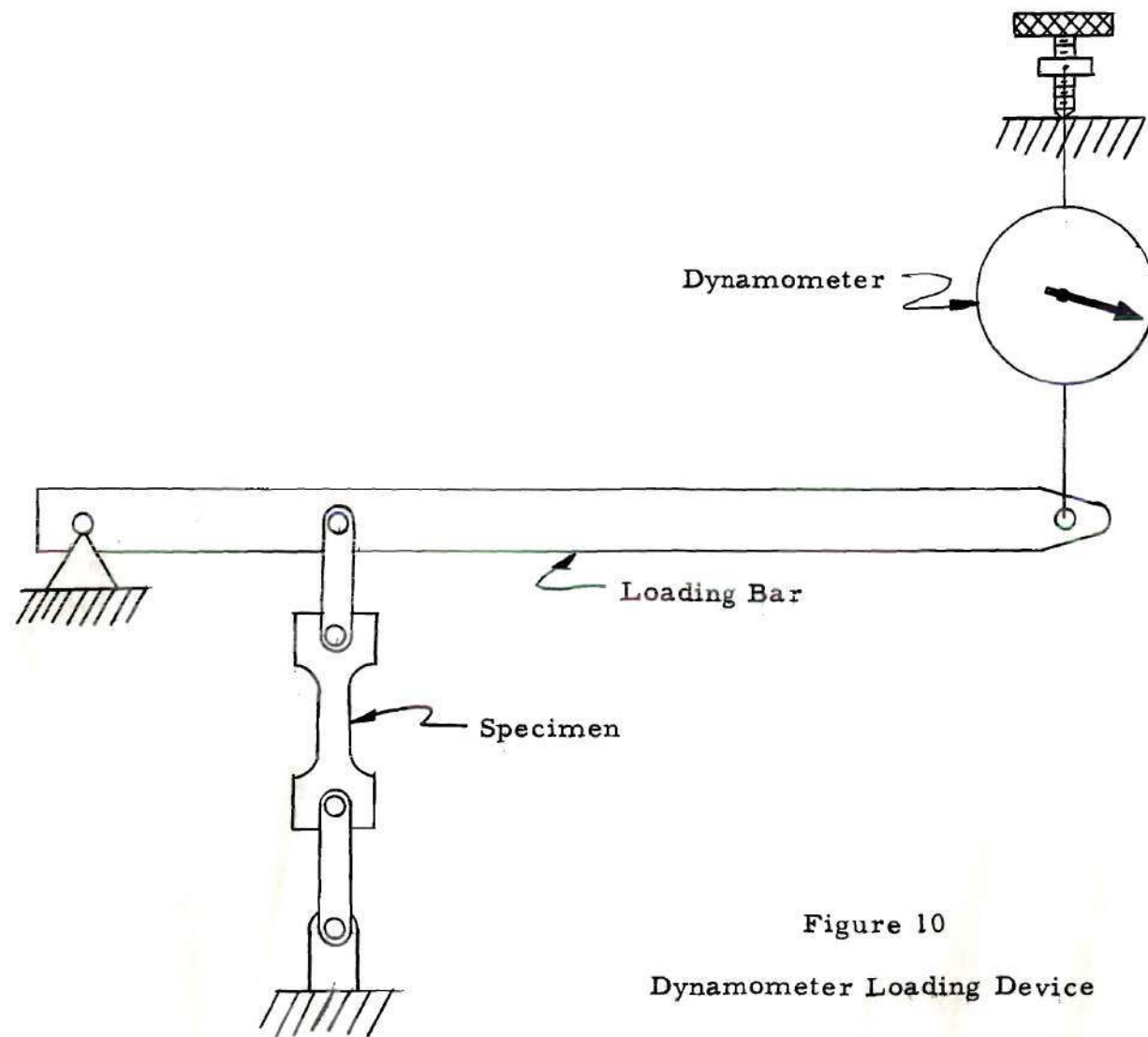


Figure 10
Dynamometer Loading Device

pulley, giving the bar an upward motion. A screw jack at the top of the loading frame was used to apply load and movement to the loading bar for the creep balance and dynamometer tests. This screw transmitted force to the loading bar, either directly with a chain or with a dynamometer inserted between the screw and bar. The load could be obtained directly from the dynamometer but could not be ascertained for the constant strain device. A series of linkages with ball bearing pin joints distributed the load in the required manner to the specimen. The study of each specimen was confined to either one or two points, depending on the type of specimen. Since the fringe values had to be read at exact intervals of time readings at a greater number of points was not considered feasible. Readings were taken as follows:

- (1) initially at time $t = 0$, which was always within fifteen seconds after application of load,
- (2) every three minutes until $t = 30$ minutes,
- (3) every five minutes from $t = 30$ to $t = 60$ minutes,
- (4) every ten minutes from $t = 60$ minutes to $t = 120$ minutes.

Fringe values were read by the Tardy¹ method to the nearest degree. Although the writer was somewhat dubious of his skill with the Tardy method, since it relies on visual comparison of shades, the ability to reproduce individual measurements seemed to indicate accuracy well within $\pm 3^\circ$ of analyzer rotation for fringe orders as high as five. This would give an accuracy within .03 fringes. Fringe orders were kept well within the elastic range of CR-39 except very near the loading points where stress concentrations occurred.

¹Details of this method are given in reference (4), p. 40.

No isoclinic measurements were made since the models used were standard types with isoclinic patterns readily available in the literature.

No relaxation data was recorded but visual inspection revealed severe residual stresses as high as $1\frac{1}{2}$ fringes immediately upon unloading. Some residual stress was still apparent 18 to 30 hours after unloading the specimens.

CHAPTER V

DISCUSSION OF RESULTS

Creep results are compared as per cent of fringe value, the value thirty minutes after application of the load being considered one hundred per cent. Some such definition is necessary because of the variance in model dimensions and the impossibility of reproducing the exact loading from test to test. Since some degree of stabilization in creep is necessary to arrive at an accurate basis for comparison, and since the creep rate is very rapid for several minutes following loading, thus reducing the accuracy of the reading, the fringe value at thirty minutes has arbitrarily been chosen as the basis for comparison. Curves showing per cent of fringe order versus time may be found in the appendix. The points on the curves are numerical averages of three tests of equal weight. A discussion of the curves follows.

Beam in Pure Bending.—Readings for beams in pure bending were taken at two points approximately $1/16$ inch from the edge of the specimen, one on the tensile side, the other on the compressive side. No appreciable difference in creep rates was noted between the tensile and compressive sides of the beam in any test. The total creep observed for the constant load specimens was much greater than for the constant strain and dynamometer tests, the results of which were almost identical.

Beam with Concentrated Load.—Like the beam in pure bending no significant difference was noted in creep rates on tensile and compressive sections of the beams. Total creep for the constant loading was much greater than for the other two types of loading. The constant strain loading exhibited the smallest amount of creep, varying only slightly more than one per cent for the two hour test.

Tensile Member.—Readings were taken at one point, in the center, of the tensile specimens. No significant difference in creep rates was noted among these tests. A fringe reduction phenomena was first recorded in these tests with the constant strain loading mechanism. On test C-8 the fringe order decreased from 3.78 at 24 minutes to 3.72 at 35 minutes. None of the other tests in this series exhibited this phenomenon. One explanation would be slippage in the loading mechanism. The change is not abrupt, however, and the author does not believe that this hypothesis warrants acceptance without further proof.

Curved Beam.—Results of these tests were disconcerting. For instance, with the constant strain device the fringe order decreased as much as two percent during the first three minutes of the test. The fringe reduction phenomenon was observed in both tensile and compressive stress areas of specimens D-1, D-2, and D-3. A slight effect of this type was noted on tests D-4, D-5, and D-6 which were loaded with a dynamometer. No such effect was seen on the constant load tests. These results seem to indicate that plastic flow was occurring near the loading pin holes. While this conclusion may cause the

validity of these tests to be questioned, it must be remembered that the models used here are types previously used in the laboratory and the curves represent actual creep conditions that may occur with a specific specimen and type of loading.

Although irregular curves were obtained for constant strain and dynamometer loading the total creep range was much less than for the constant load test, being a maximum of three per cent, four per cent, and fifteen per cent respectively.

Radially Loaded Disk.—Fluctuations in fringe reading for the radially loaded disks were so large that no firm conclusions may be drawn. It is noteworthy, however that during the first few minutes there is a marked reduction in the initial fringe order of the constant strain specimens. These tests may substantiate the hypothesis of plastic yielding at the loading points.

CHAPTER VI

CONCLUSIONS

A theoretical analysis of three types of loading methods for photoelastic models has shown that:

- (1) a constant load on a model will produce a constant fringe pattern only if the retardation is independent of strain,
- (2) a constant strain loading device will produce a constant fringe pattern only if the retardation is independent of stress,
- (3) a dynamometer loading device will reduce the optical creep effects dependent on stress or strain but cannot eliminate the effects due to these causes. The degree of reduction is dependent on the photoelastic material.

All three methods have been experimentally tested with a limited number of tests on laboratory models using CR-39 as a photoelastic material. It was found that both the dynamometer and constant strain devices reduced optical creep during a two hour test period from as much as fifteen per cent of the fringe order, measured with a constant load, to as low as three per cent of the fringe order. In no case did the constant load device have a lower optical creep rate than either of the other two methods. Variations of the creep rates were such that no quantitative estimate of optical creep to be expected with different model types could be made.

The optical creep rates measured with the dynamometer and constant strain devices were comparable for the model types tested. After the initial thirty minute period the creep observed with the two methods for the remainder of the two hour test was approximately one per cent on all tests. No tests were run to investigate the variation of these effects with different photoelastic materials.

Although the two methods give comparable creep results and are both preferable from this standpoint to the constant load device, the simplicity of the dynamometer device would make its use more advantageous. Use of a constant strain device would require the use of a calibration model in the system to obtain instantaneous values of the fringe coefficient. The use of the dynamometer would allow instantaneous values of the load to be recorded directly from a scale, simplifying the procedure and allowing less opportunity for error. It should be possible to provide a dynamometer, accurate to the same order of magnitude as the friction in the loading system.

CHAPTER VII

RECOMMENDATIONS

Further work with this topic may well proceed along the following lines:

- (1) similar investigations with other photoelastic materials,
- (2) investigation of the effects on optical creep of high stress concentration at loading points,
- (3) investigation of the correlation of physical creep with optical creep, using the three loading mechanisms discussed here,
- (4) investigation of the dependence of physical creep rate on stress for various photoelastic materials.

It is believed that the investigation of creep rates of new materials holds much promise, due to the continually increasing numbers of new plastics introduced.

APPENDIX

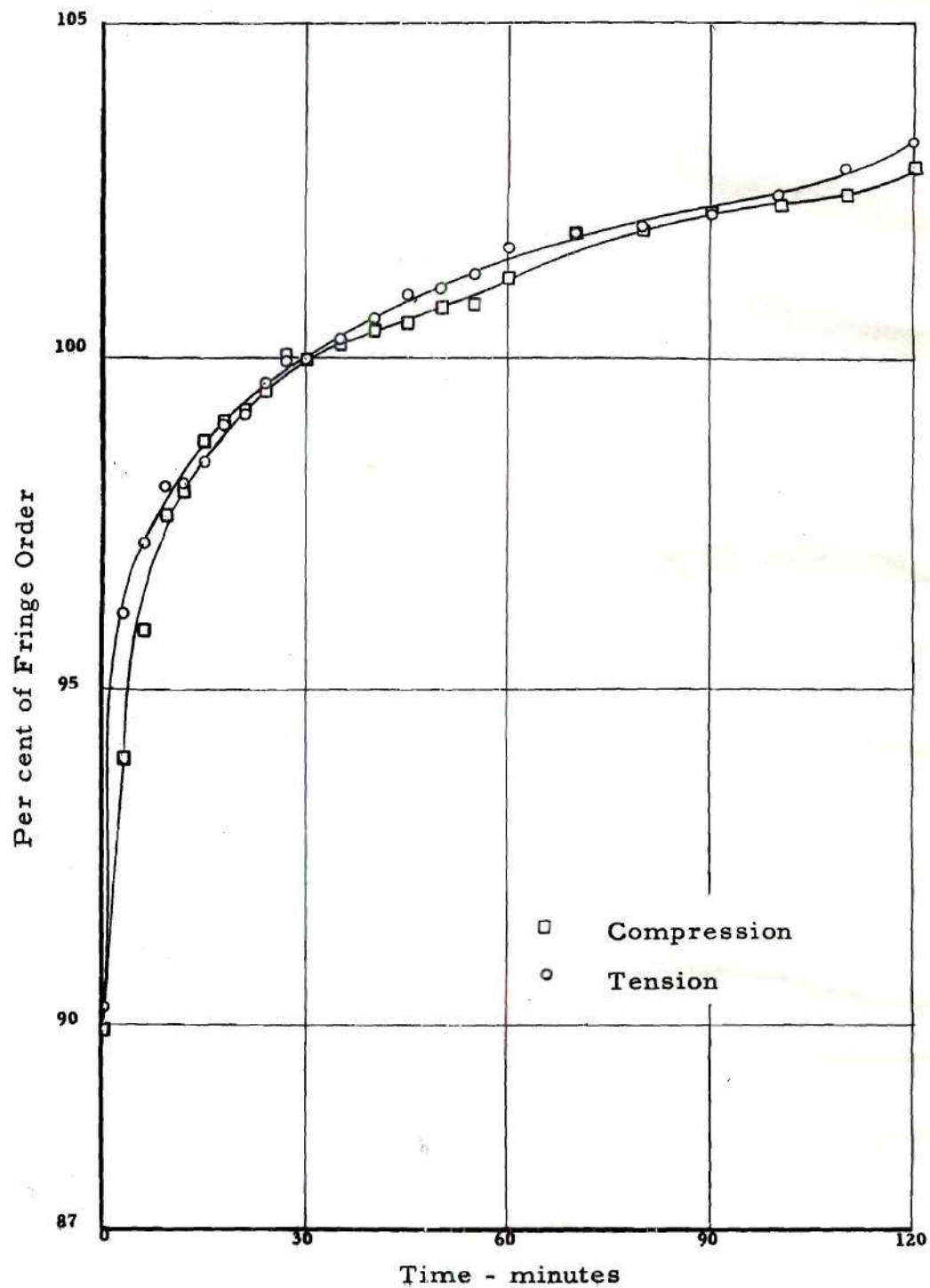


Figure 11. Optical Creep of Beam in Pure Bending, Constant Load
Specimens A-3, A-4, A-9

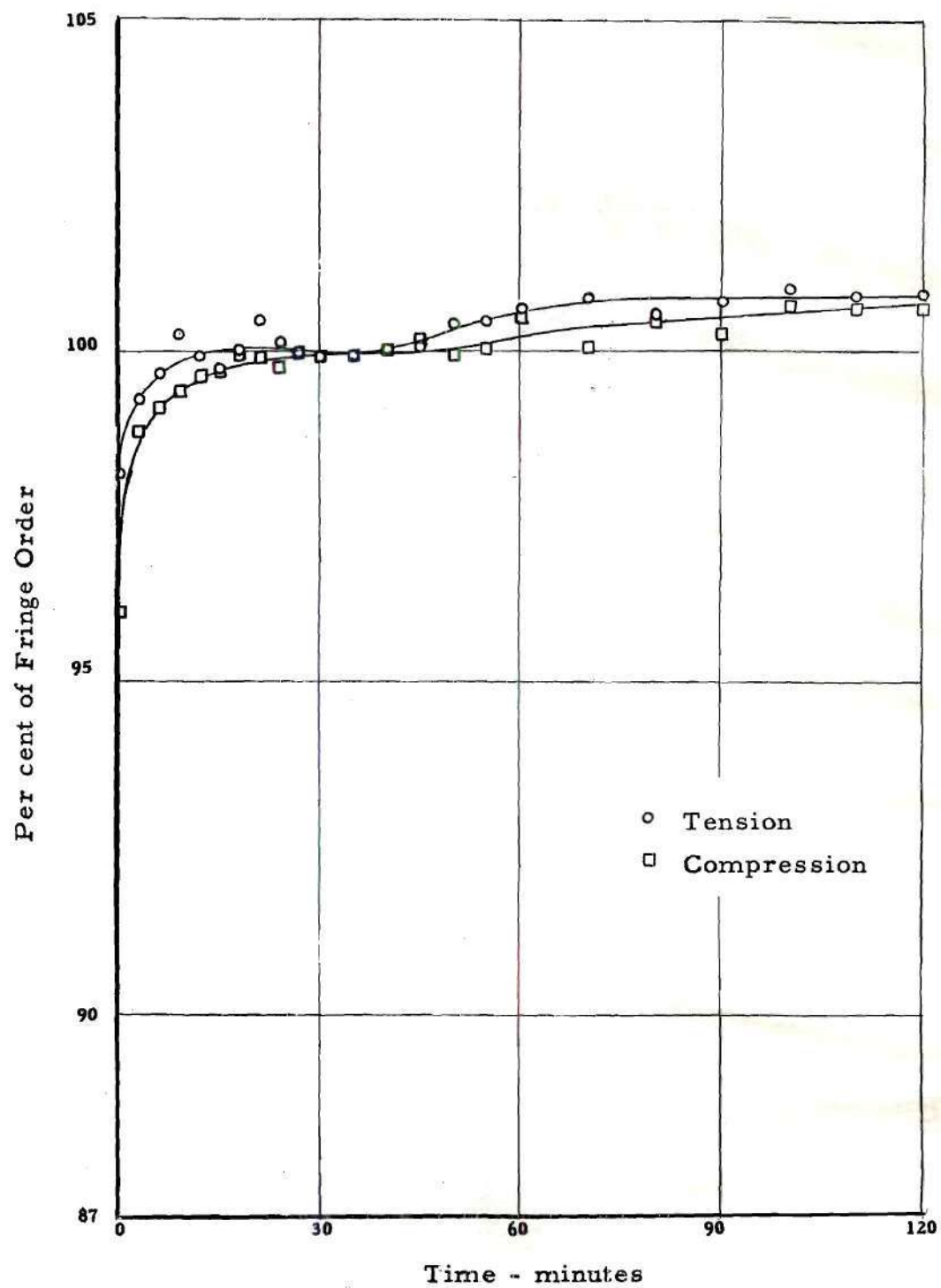


Figure 12. Optical Creep of Beam in Pure Bending, Constant Strain
Specimens A-5, A-7, A-8

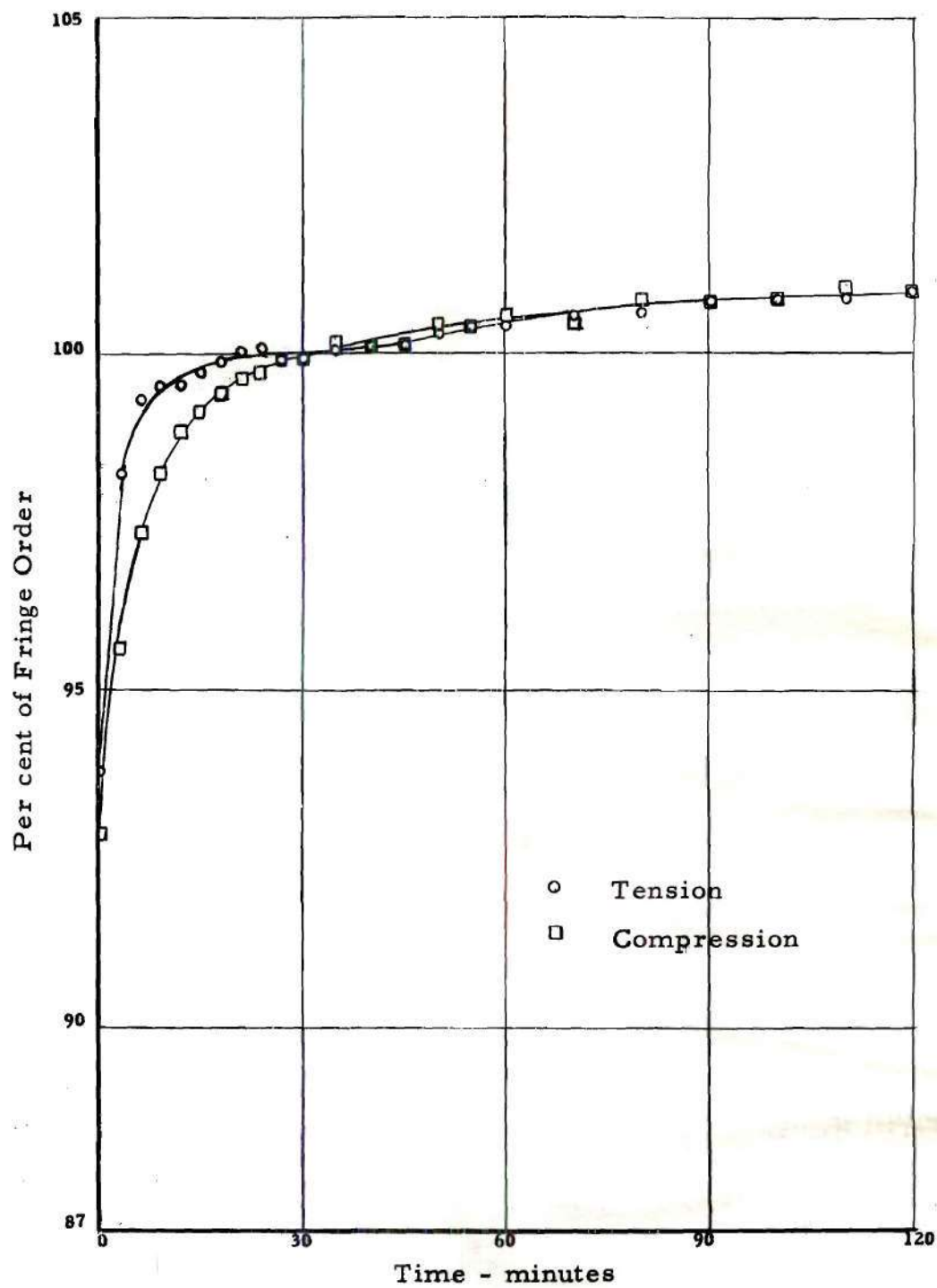


Figure 13. Optical Creep of Beam in Pure Bending, Dynamometer Load
Specimens A-11, A-12, A-13

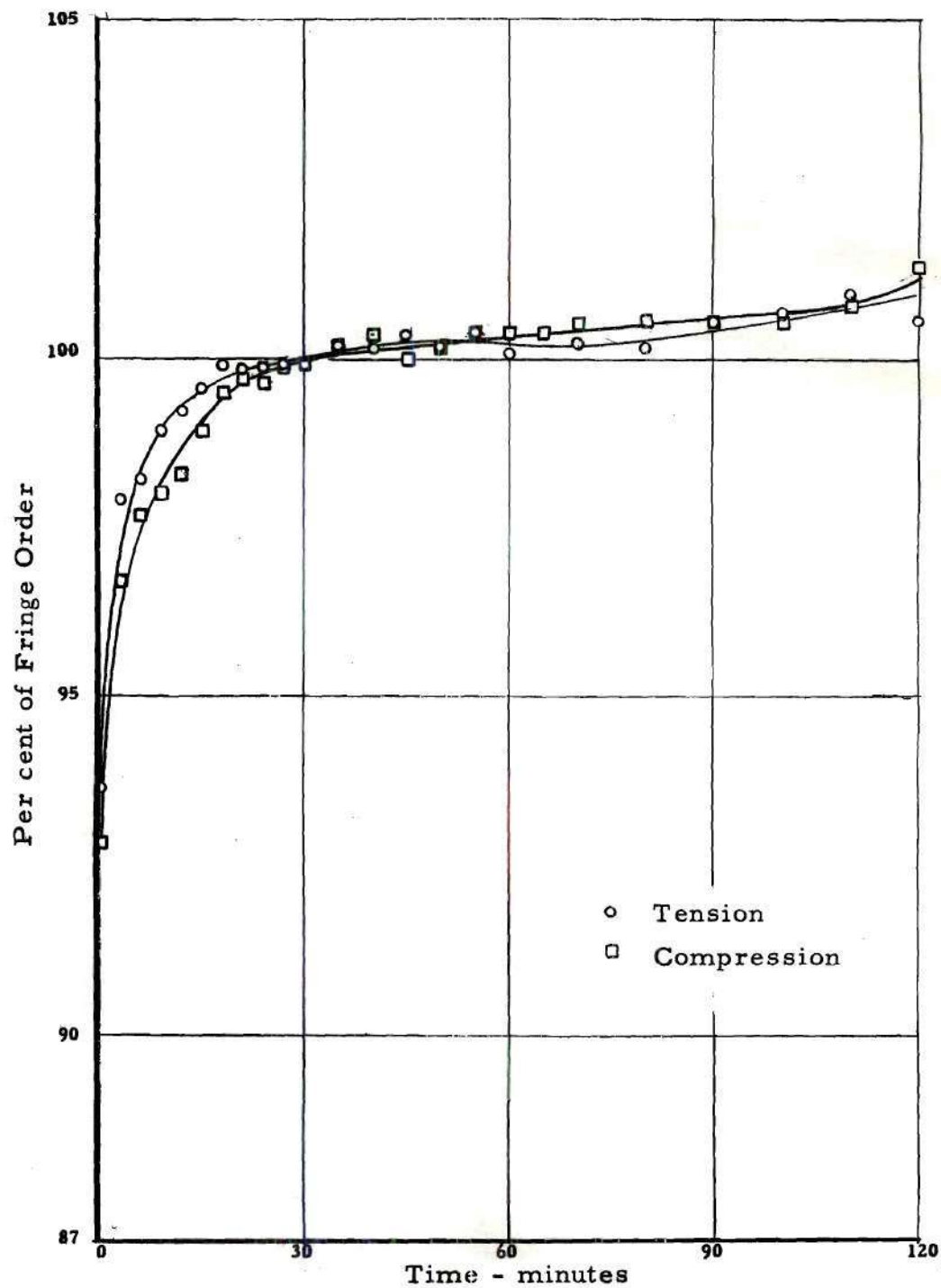


Figure 14

Optical Creep of Beam With Concentrated Load, Dynamometer Load
Specimens B-1, B-3, B-4

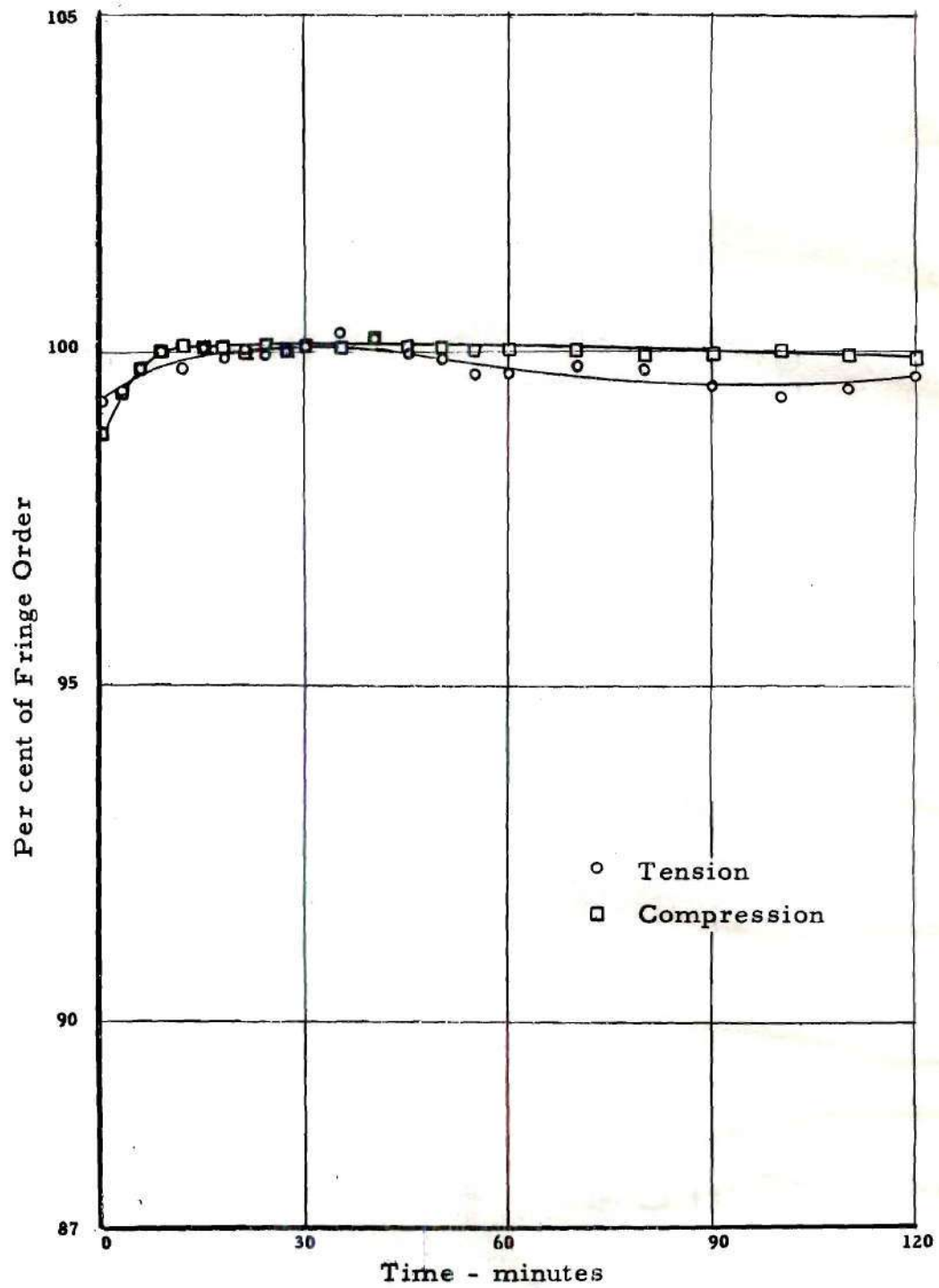


Figure 15
Optical Creep of Beam, Concentrated Load, Constant Strain
Specimens B-5, B-6, B-7

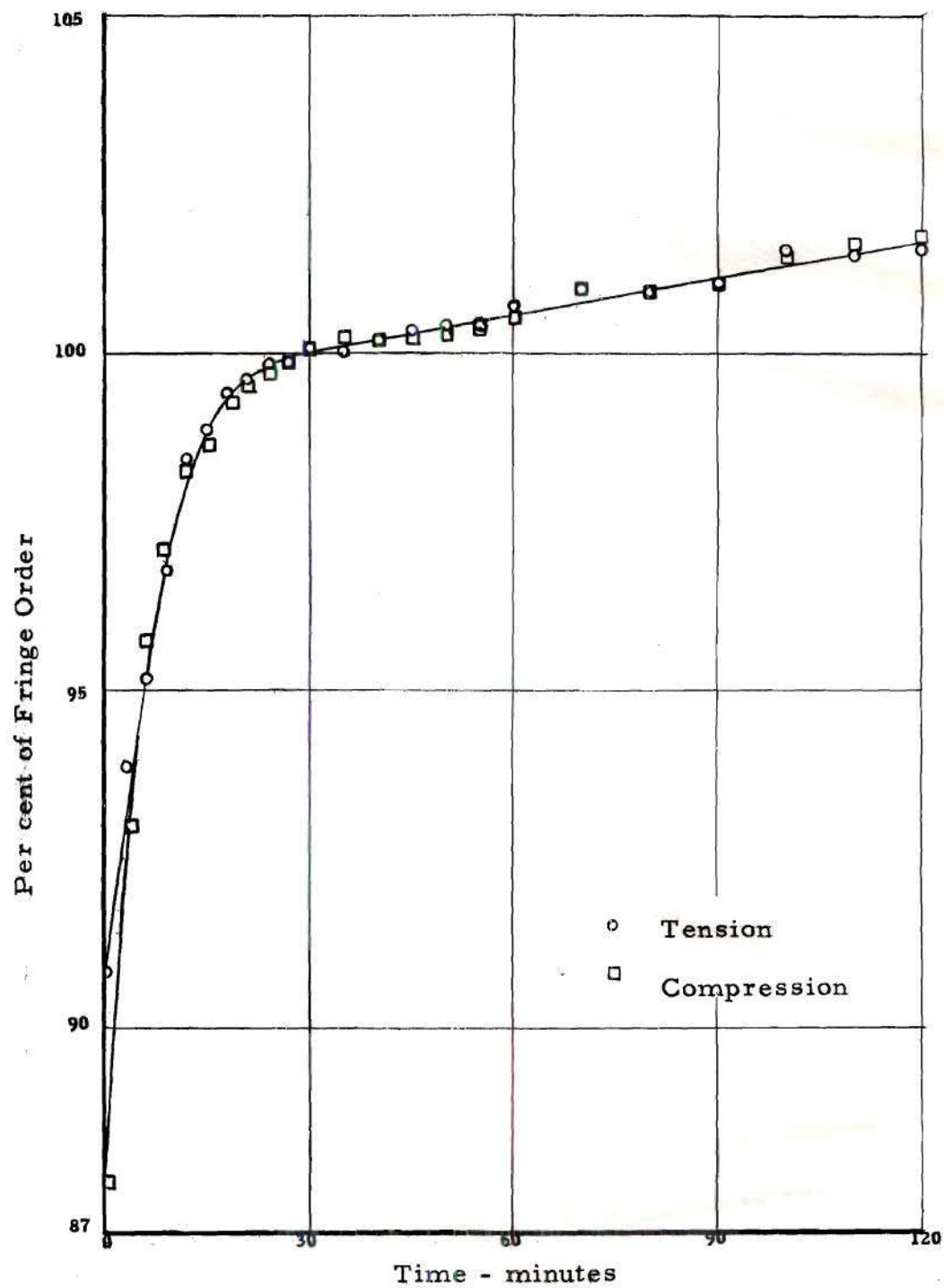


Figure 16
Optical Creep of Beam With Concentrated Load, Constant Load
Specimens B-10, B-11, B-12

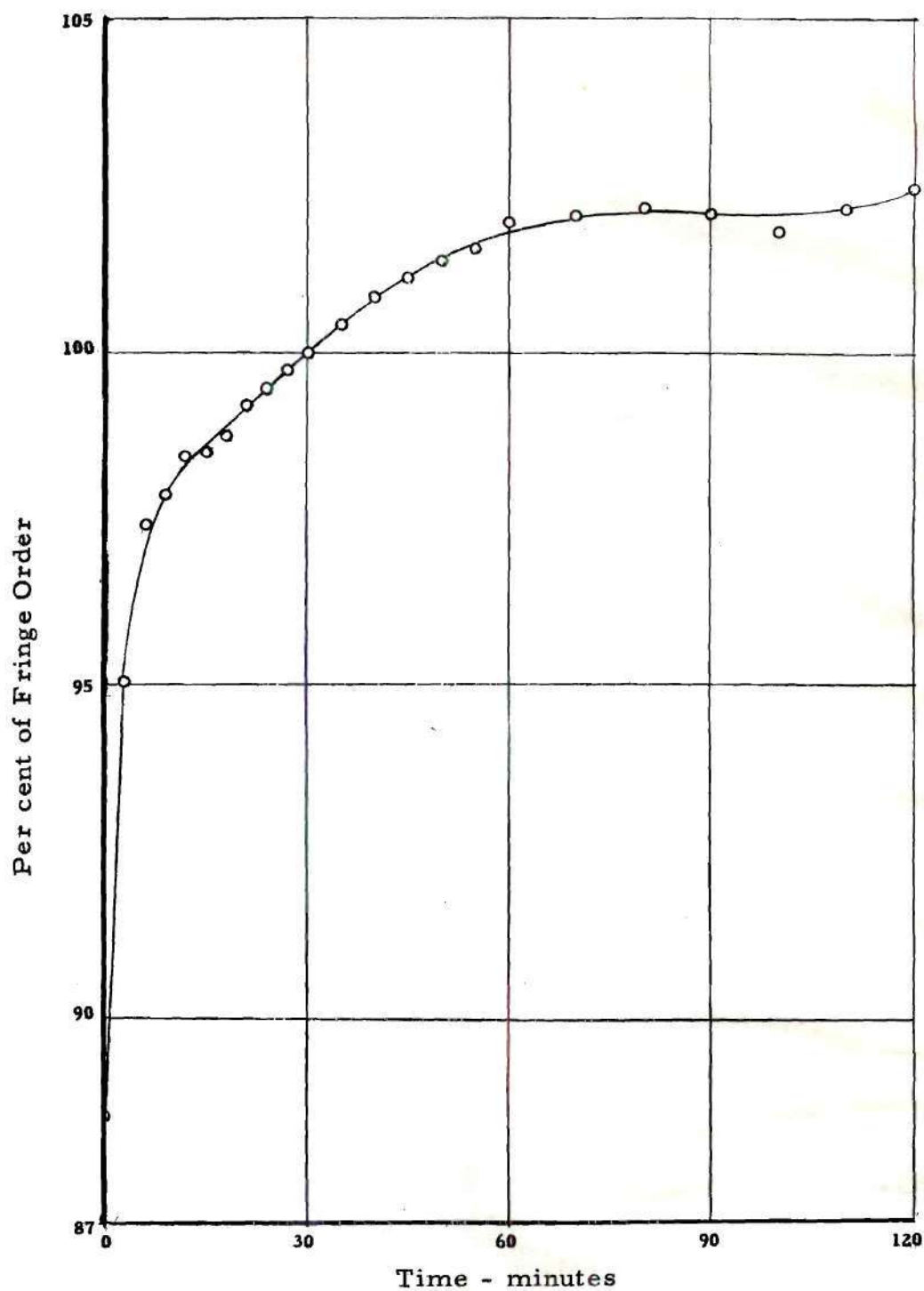


Figure 17. Optical Creep of Tensile Bar, Constant Load
Specimens B-5, B-6, B-7

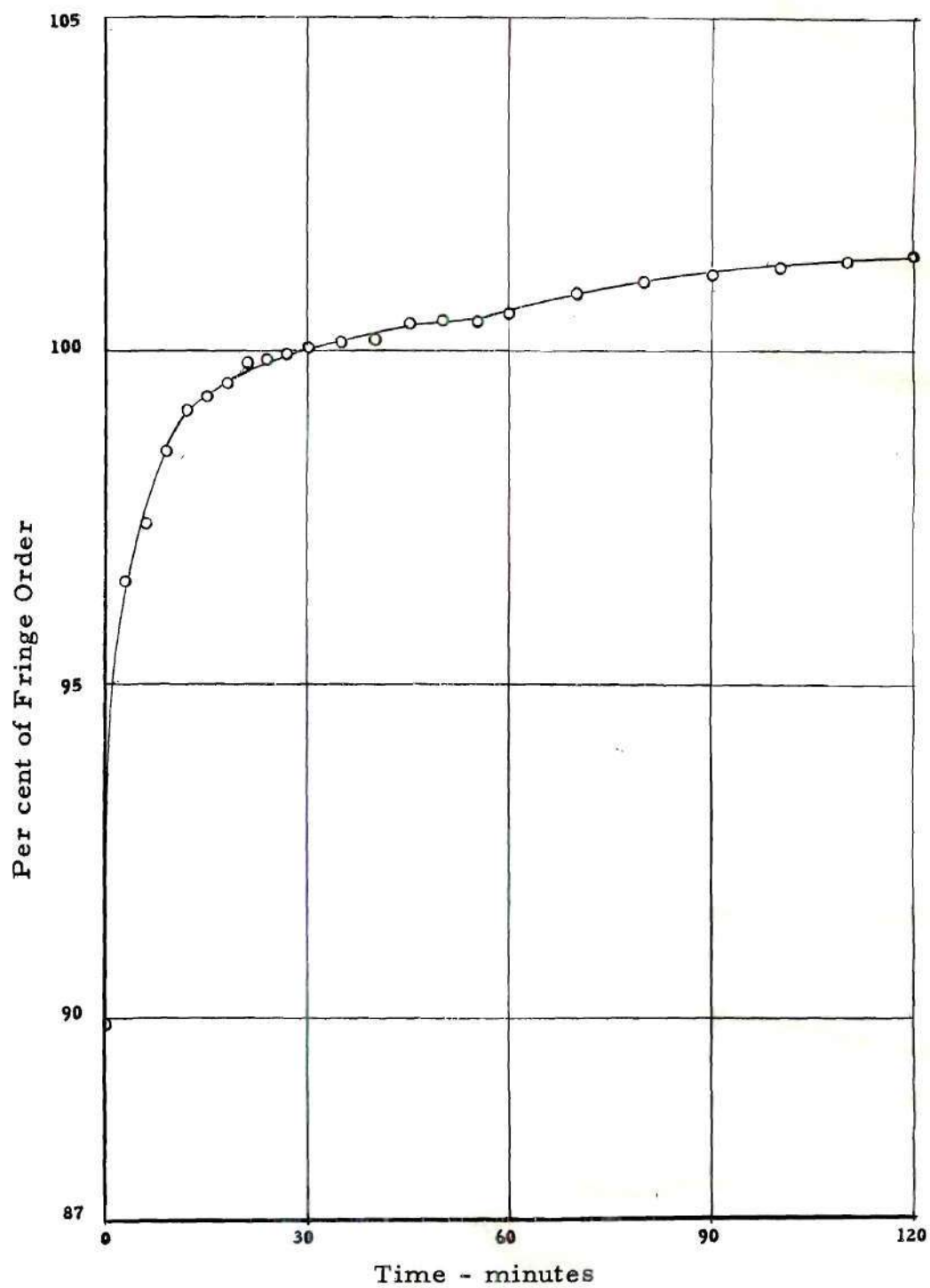


Figure 18. Optical Creep of Tensile Bar, Dynamometer Load
Specimens C-5, C-6, C-7

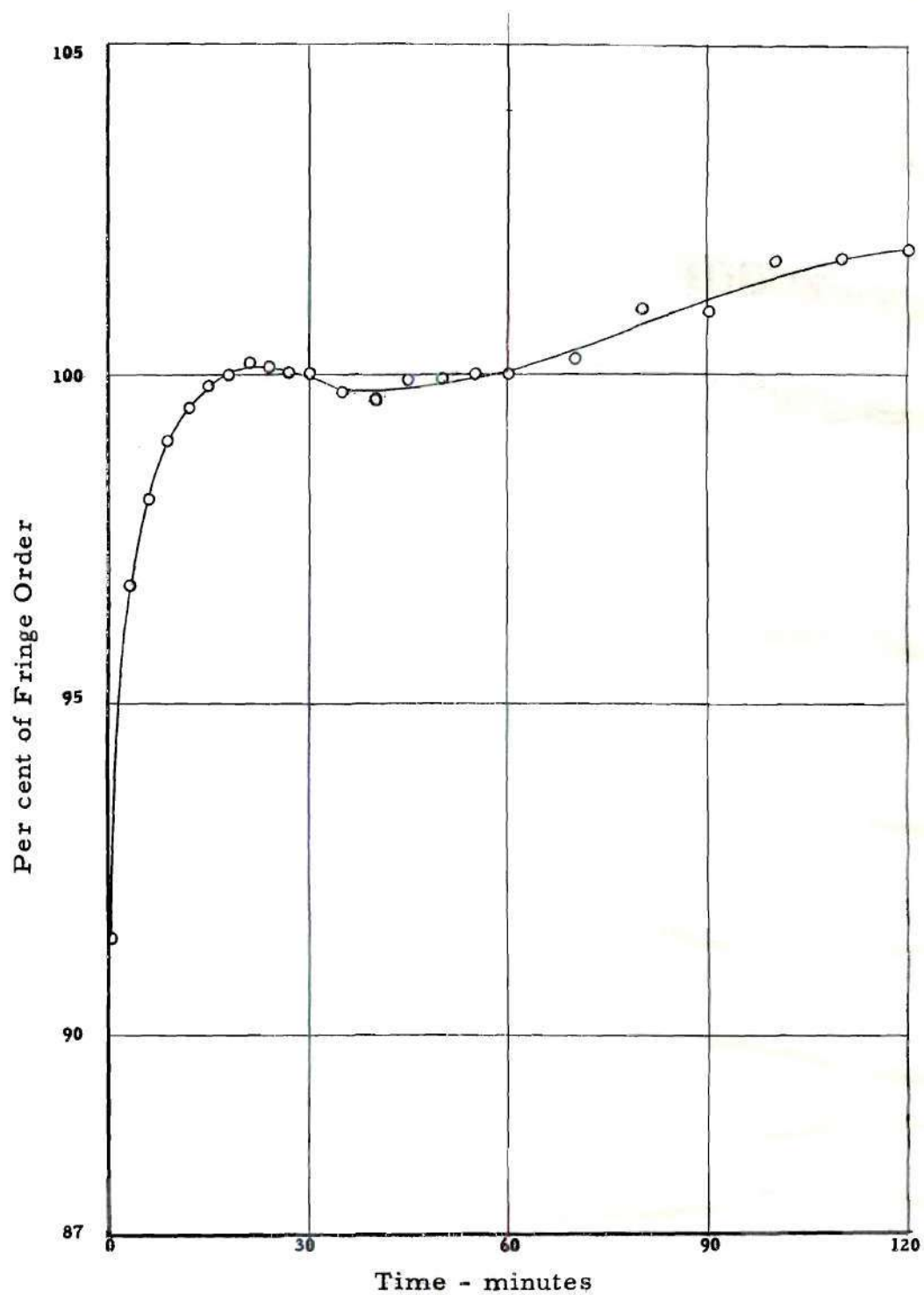


Figure 19. Optical Creep of Tensile Bar, Constant Strain
Specimens C-8, C-9, C-10

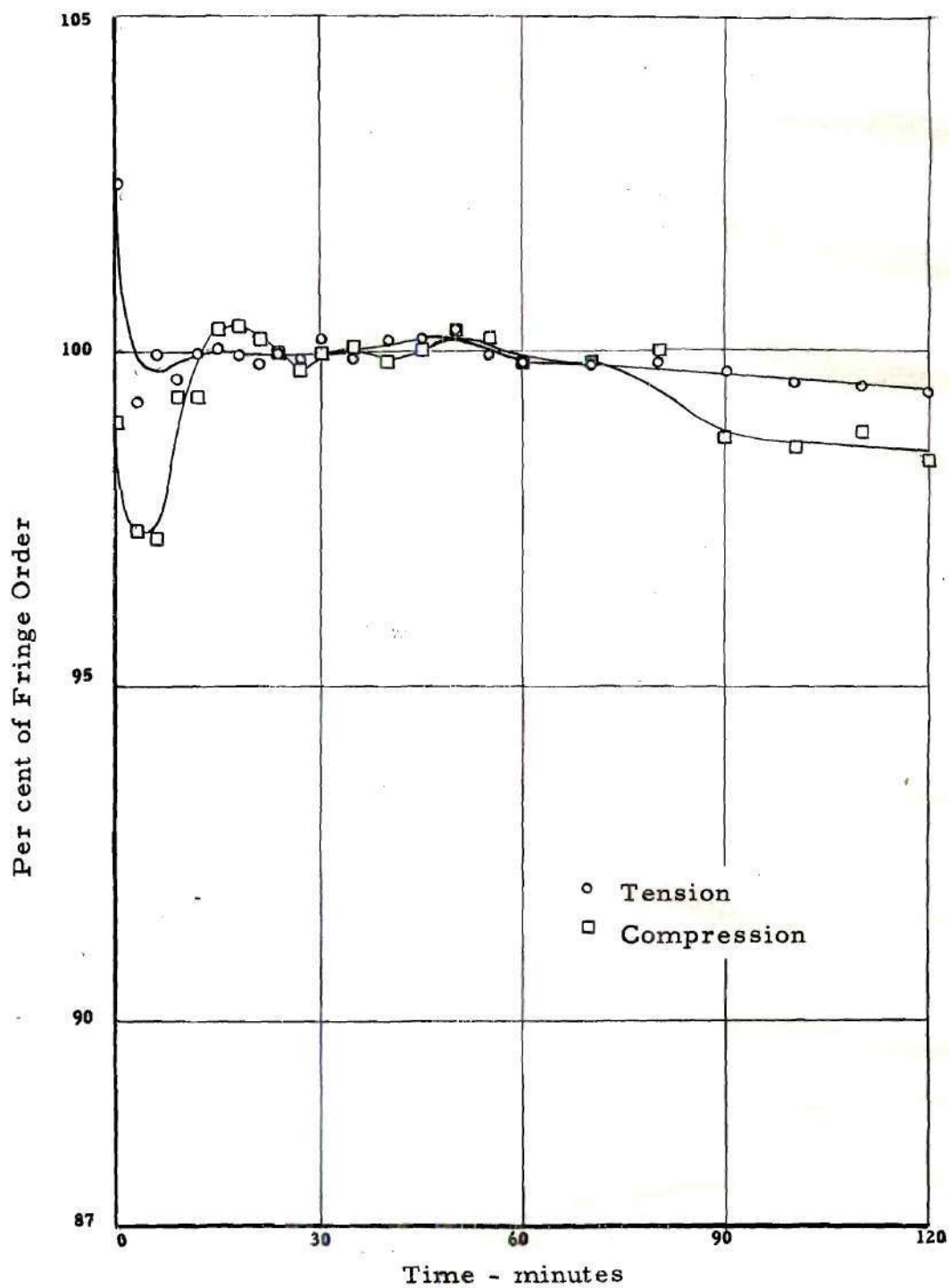


Figure 20. Optical Creep of Curved Beam, Constant Strain
Specimens D-1, D-2, D-3

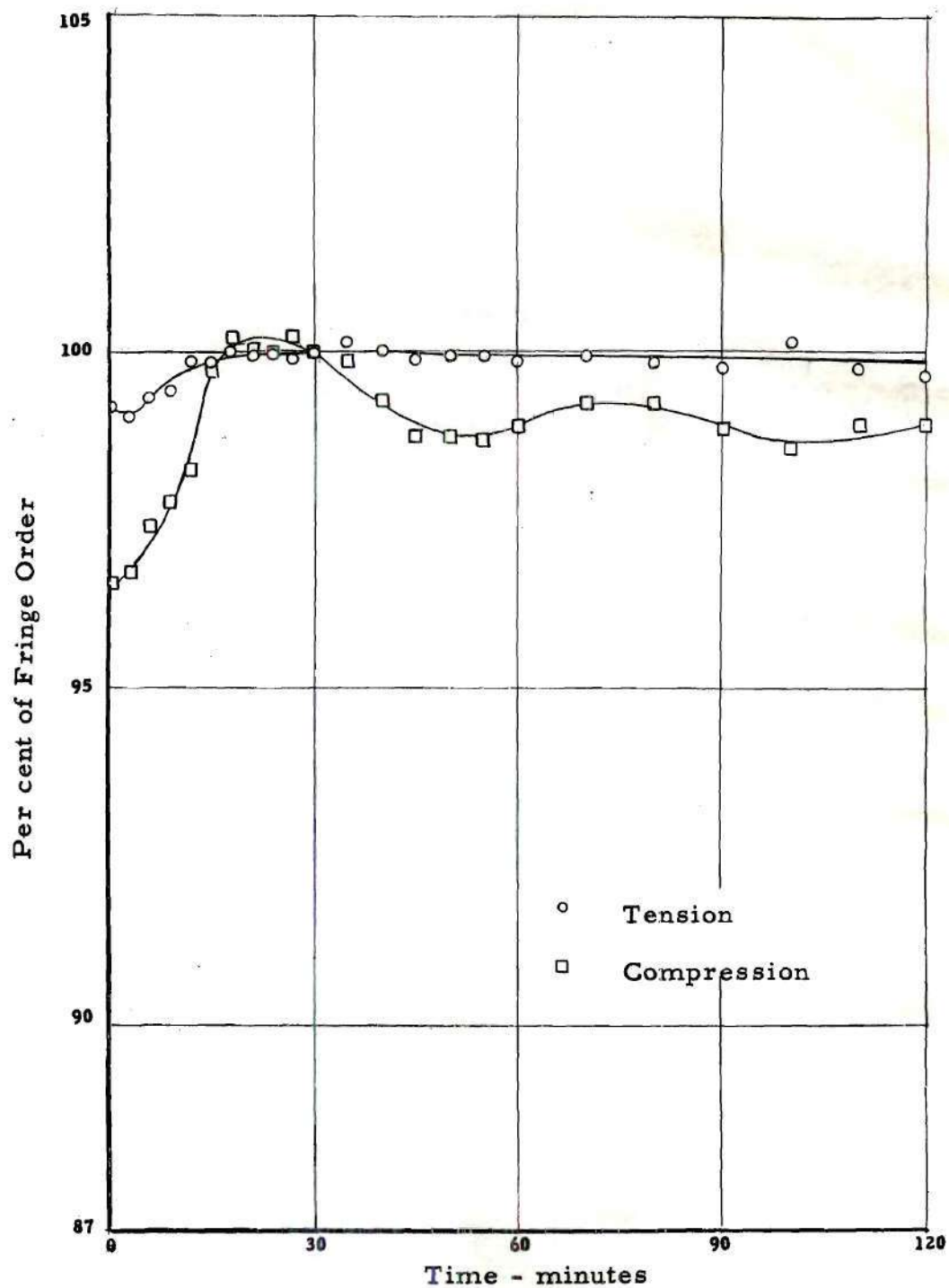


Figure 21. Optical Creep of Curved Beam, Dynamometer Load
Specimens D-4, D-5, D-6

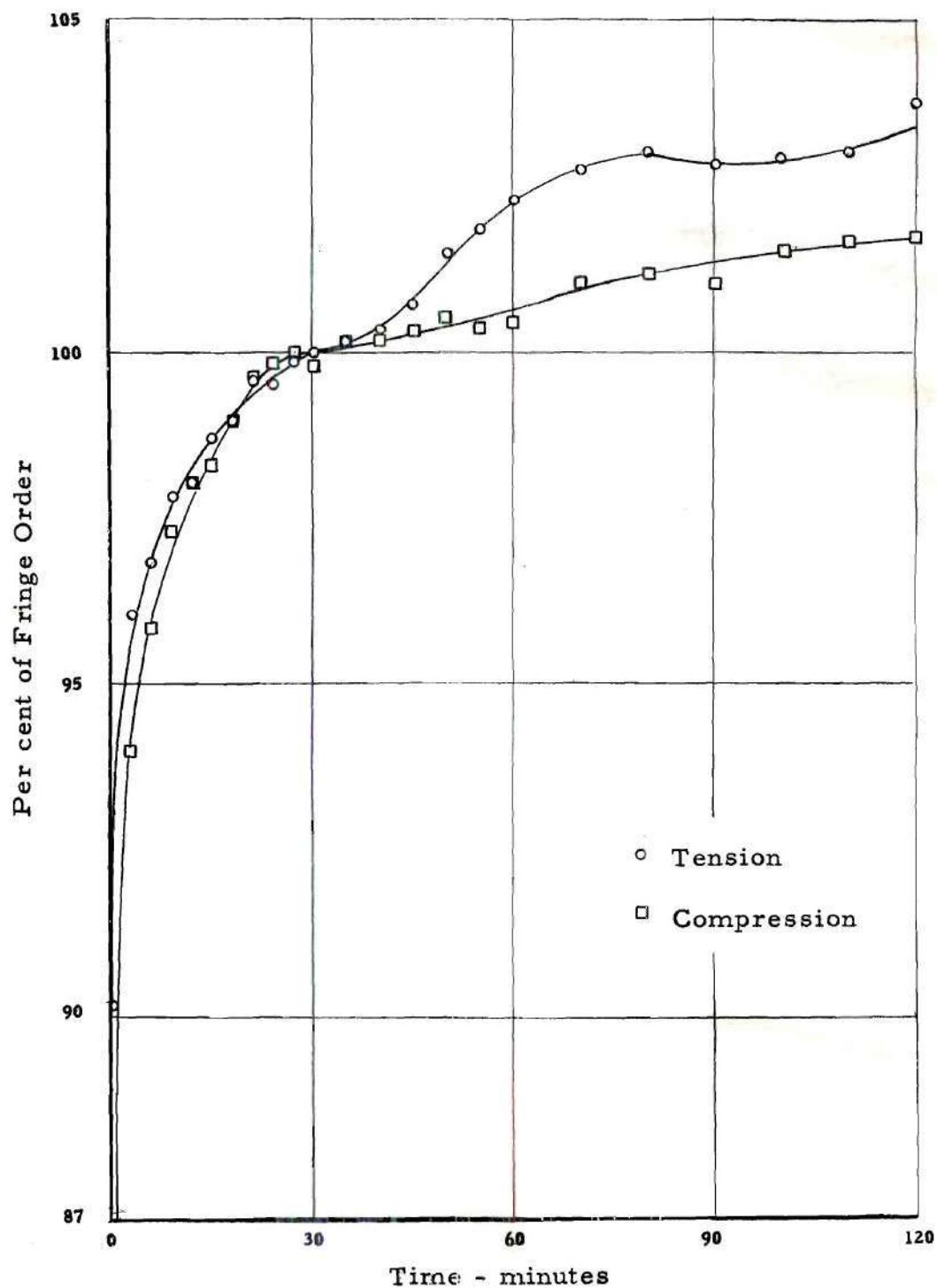


Figure 22. Optical Creep of Curved Beam, Constant Load
Specimens D-7, D-8, D-9

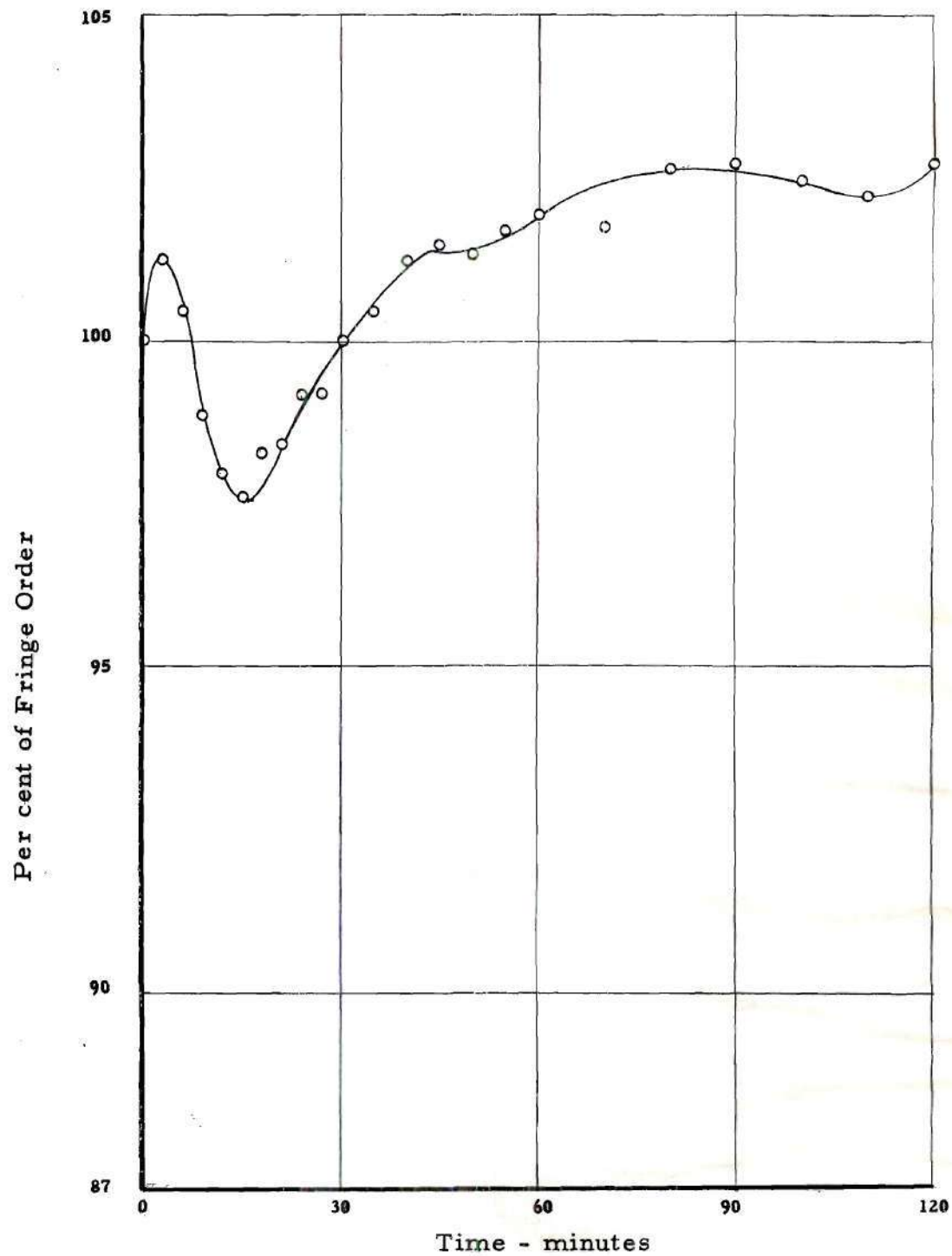


Figure 23. Optical Creep of Disk in Compression, Constant Load
Specimens E-1, E-2, E-3

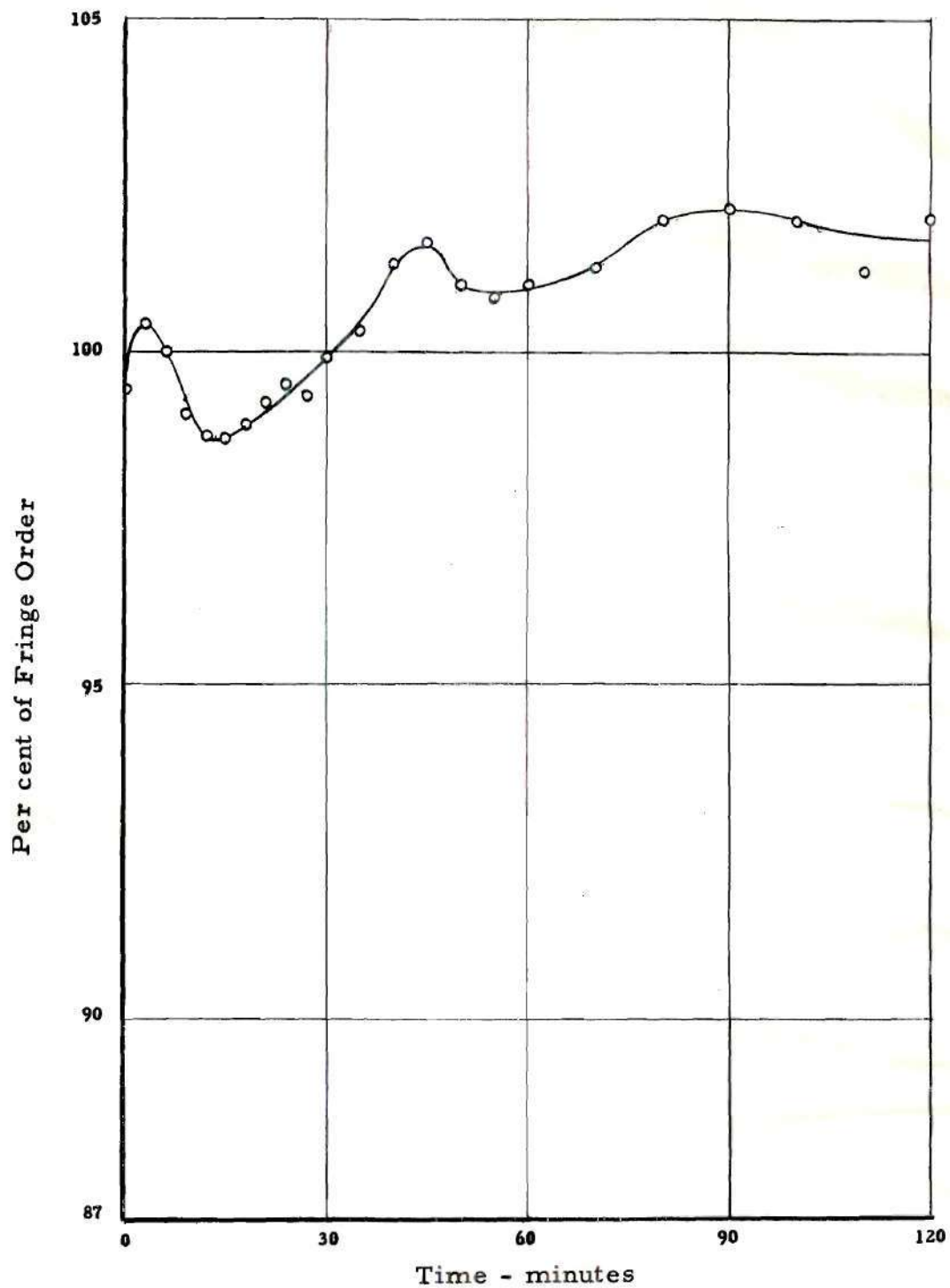


Figure 24. Optical Creep of Disk in Compression, Dynamometer Load Specimens E-4, E-5, E-6

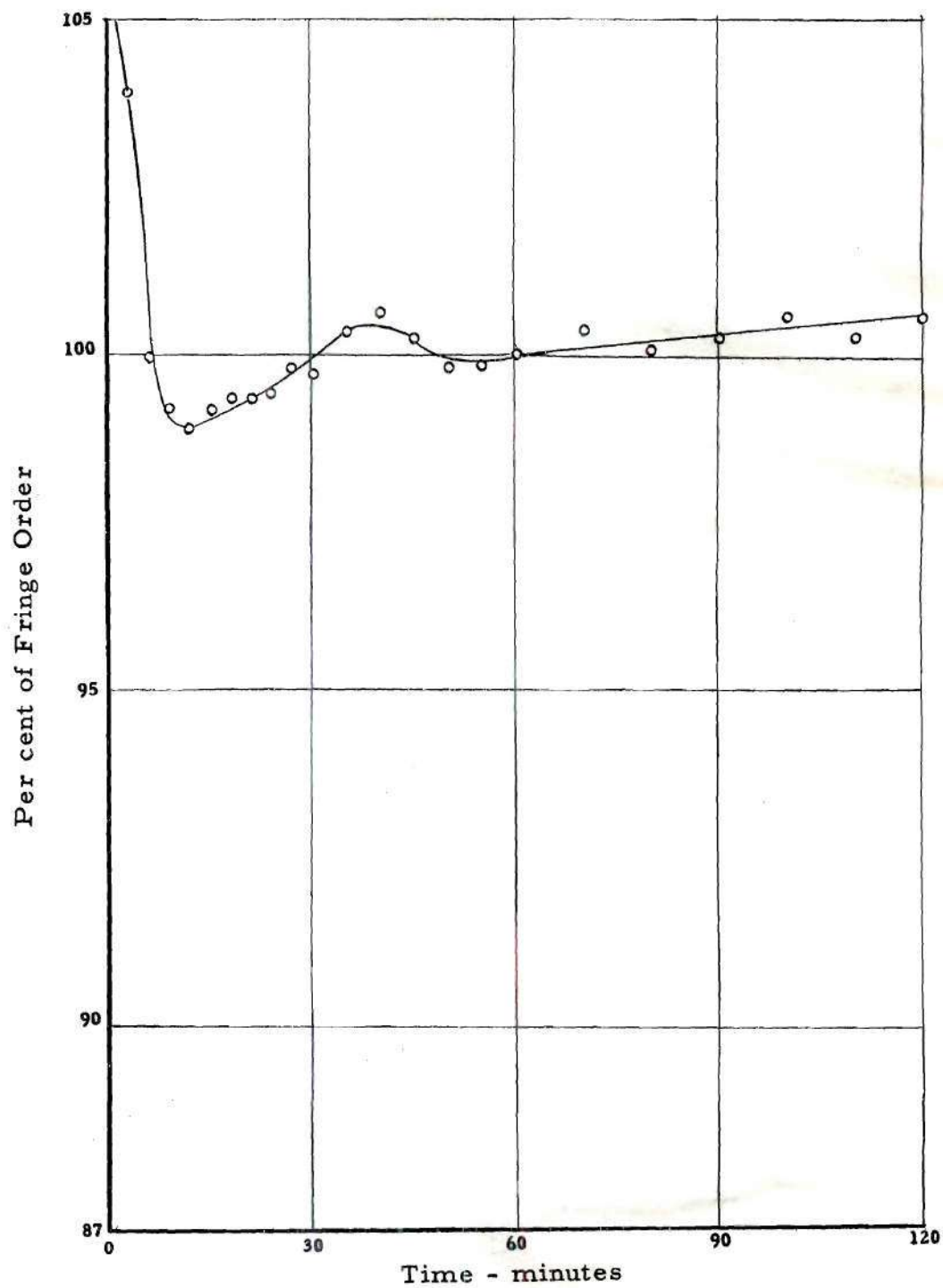


Figure 25. Optical Creep of Disk in Compression, Constant Strain
Specimens E-7, E-8, E-9

TABLE 1

Optical Creep of Beam in Pure Bending, Constant Load
Specimens A-3, A-4, A-9

Time After Loading (min.)	Fringe Reading as Per Cent							
	Tensile Field				Compressive Field			
	A-3	A-4	A-9	Average	A-3	A-4	A-9	Average
0	85.81	91.61	93.45	90.29	88.01	88.19	93.57	89.92
3	93.80	97.00	97.59	96.13	90.71	93.79	97.51	94.00
6	94.73	98.34	98.67	97.25	93.44	95.68	98.38	95.83
9	95.98	99.16	99.20	98.11	97.29	96.66	99.00	97.65
12	95.98	98.68	99.86	98.17	97.62	97.31	99.11	98.01
15	96.66	99.16	99.59	98.47	98.76	98.48	99.00	98.75
18	98.27	99.16	99.59	99.01	99.21	98.48	99.73	99.14
21	98.39	99.53	99.59	99.17	98.98	99.28	99.62	99.29
24	99.53	99.87	99.59	99.66	99.33	99.28	99.87	99.49
27	99.75	99.87	100.27	99.96	99.78	100.23	100.11	100.04
30	100.00	99.87	100.14	100.00	100.00	99.87	99.87	99.91
35	100.56	100.37	100.00	100.31	100.12	100.59	100.00	100.24
40	101.36	100.37	100.14	100.62	100.45	100.59	100.22	100.42
45	101.81	100.84	100.14	100.94	100.35	100.82	100.36	100.51
50	101.94	100.84	100.27	101.02	100.35	101.18	100.73	100.75
55	101.58	101.44	100.67	101.23	100.35	101.18	100.85	100.79
60	102.74	101.79	100.53	101.69	101.47	101.28	100.85	101.20
70	102.62	102.16	102.80	100.86	101.16	102.98	101.49	101.88
80	102.62	102.39	100.80	101.94	102.16	102.23	101.35	101.91
90	102.62	102.13	100.80	102.18	102.38	102.13	102.09	102.20
100	102.84	103.00	107.47	102.44	102.04	102.46	102.47	102.32
110	103.64	103.34	101.59	102.85	102.38	102.46	102.47	102.44
120	104.80	103.47	101.59	103.29	102.95	103.93	102.71	102.86
100 Per Cent Fringe Order Value								
	4.86	4.64	4.15		4.91	4.75	4.49	

TABLE 2
Optical Creep of Beam in Pure Bending, Constant Strain
Specimens A-5, A-7, A-8

Time After Loading (min.)	Fringe Reading as Per Cent						
	Tensile Field			Compressive Field			
	A-5	A-7	A-8	Average	A-5	A-7	A-8
0	99.52	97.31	97.68	98.17	98.76	97.15	92.31
3	99.76	98.48	99.65	99.30	98.98	98.43	99.01
6	100.73	98.61	99.65	99.66	99.33	98.37	99.78
9	100.97	99.18	100.58	100.24	99.55	99.02	99.66
12	100.50	99.07	100.23	99.93	99.43	99.88	99.66
15	100.00	98.82	100.33	99.72	99.55	99.78	99.78
18	100.00	99.66	100.33	100.00	100.00	100.00	99.78
21	100.37	99.77	100.00	100.46	100.00	99.78	100.00
24	100.37	99.77	100.23	100.12	100.00	99.78	99.57
27	100.50	99.66	99.77	99.98	100.00	100.12	100.00
30	99.76	100.00	100.00	99.92	100.00	99.78	100.00
35	99.76	100.34	99.77	99.96	100.00	99.78	100.00
40	99.65	100.23	100.33	100.07	100.00	100.12	99.90
45	99.89	100.34	100.00	100.08	100.00	100.22	100.43
50	100.00	99.87	101.49	100.45	99.90	100.43	99.45
55	100.13	99.77	101.59	100.50	100.00	100.33	99.78
60	100.24	100.00	101.72	100.65	100.12	100.86	100.55
70	100.37	100.82	101.26	100.82	100.12	100.12	100.00
80	99.89	100.82	101.04	100.58	100.00	100.65	100.77
90	100.24	100.93	101.04	100.74	100.00	100.65	100.22
100	100.37	100.72	101.72	100.94	100.00	100.98	101.12
110	100.24	100.72	101.59	100.85	100.00	100.86	101.21
120	100.24	101.28	101.14	100.89	100.00	100.65	101.32
100 Per Cent Fringe Value							
	4.63	4.75	4.83		4.92	5.09	5.06

TABLE 3
Optical Creep Beam in Pure Bending, Dynamometer Load
Specimens A-11, A-12, A-13

Time After Loading (min.)	Tensile Field			Fringe Reading as Per Cent			Compressive Field		
	A-11	A-12	A-13	Average	A-11	A-12	A-13	Average	
0	91.94	96.09	93.30	93.78	91.92	92.29	94.43	92.88	
3	96.73	99.35	98.69	98.26	93.38	97.85	95.82	95.68	
6	98.16	99.35	100.56	99.36	97.00	97.96	97.21	97.39	
9	98.47	99.78	100.34	99.53	98.23	98.55	97.96	98.25	
12	98.69	99.78	100.12	99.53	98.97	98.55	99.13	98.88	
15	99.24	100.00	100.00	99.75	99.27	98.78	99.46	99.17	
18	99.67	99.90	100.12	99.90	99.27	99.07	99.88	99.41	
21	99.90	100.22	100.00	100.04	99.91	99.30	99.67	99.63	
24	99.90	100.12	100.12	100.05	99.59	99.80	99.88	99.76	
27	100.12	99.90	99.90	99.97	99.59	100.00	99.67	99.75	
30	99.90	100.12	99.90	99.97	100.00	100.00	99.79	99.93	
35	100.00	100.12	100.00	100.04	99.91	100.00	100.71	100.20	
40	100.12	99.90	100.34	100.12	100.21	100.20	100.00	100.12	
45	100.00	99.90	100.56	100.15	99.68	100.11	100.33	100.04	
50	100.00	100.43	100.67	100.37	100.32	100.52	100.64	100.49	
55	100.12	100.33	100.89	100.45	100.21	100.43	100.64	100.43	
60	100.00	100.43	100.89	100.44	100.21	100.43	101.17	100.60	
70	100.43	100.55	100.89	100.62	100.21	100.43	100.87	100.50	
80	100.65	100.43	100.77	100.62	100.52	100.72	101.06	100.77	
90	100.65	100.55	101.23	100.81	100.32	100.43	101.60	100.78	
100	100.55	100.43	101.55	100.84	100.52	100.81	101.29	100.87	
110	100.43	100.76	101.33	100.84	100.73	100.95	101.39	101.02	
120	100.55	100.76	101.45	100.92	100.93	100.81	101.16	100.97	
100 Per Cent Fringe Value									
	5.10	5.11	5.04		5.36	5.39	5.89		

TABLE 4
Optical Creep Beam, Concentrated Load, Dynamometer Load
Specimens B-1, B-3, B-4

Time After Loading (min.)	Fringe Reading as Per Cent						
	Tensile Field			Compressive Field			
	B-1	B-3	B-4	Average	B-1	B-3	B-4
0	94.07	95.47	91.43	93.66	94.00	92.73	92.08
3	99.49	97.33	96.97	97.93	97.85	95.42	97.07
6	99.49	96.67	98.57	98.24	97.85	97.07	98.20
9	99.38	97.52	100.00	98.96	98.45	97.36	98.37
12	99.38	98.35	100.00	99.24	98.67	97.66	98.84
15	99.58	99.20	100.00	99.59	99.18	98.84	98.84
18	99.89	99.88	100.00	99.92	99.58	99.76	99.19
21	99.82	99.72	100.00	99.85	99.98	99.60	99.80
24	99.89	99.88	99.86	99.88	99.78	99.43	99.65
27	99.58	100.58	99.69	99.95	99.78	100.03	99.80
30	99.69	100.06	100.00	99.92	99.98	99.89	100.00
35	100.00	100.58	100.00	100.19	99.78	100.78	100.00
40	100.00	100.58	99.86	100.15	99.98	100.51	100.46
45	100.18	100.58	100.31	100.36	99.98	100.51	99.51
50	100.18	99.88	100.49	100.18	100.18	100.94	99.51
55	100.31	100.58	100.31	100.40	99.98	100.35	99.80
60	100.40	99.57	100.31	100.09	100.18	100.78	100.15
70	100.31	100.06	100.31	100.22	100.18	100.78	100.15
80	100.40	99.72	100.31	100.14	100.18	101.10	100.29
90	100.99	100.43	100.31	100.58	100.18	101.10	100.46
100	100.68	100.73	100.63	100.68	99.98	101.24	100.46
110	100.40	101.77	100.63	100.93	100.27	101.37	100.96
120	100.49	100.92	100.31	100.57	100.18	102.29	101.60
100 Per Cent Fringe Order							
	5.54	3.27	3.50		5.49	3.71	3.45

TABLE 5
Optical Creep, Beam, Concentrated Load, Constant Strain
Specimens B-5, B-6, B-7

Time After Loading (min.)	Fringe Reading as Per Cent							
	Tensile Field				Compressive Field			
	B-5	B-6	B-7	Average	B-5	B-6	B-7	Average
0	99.52	98.81	98.51	99.28	97.79	99.15	99.05	98.73
3	99.52	99.33	99.41	99.42	99.26	99.75	99.45	99.47
6	99.83	99.48	100.00	99.77	99.42	100.00	99.72	99.71
9	99.69	99.74	100.58	100.00	99.84	99.89	100.00	99.91
12	99.69	99.60	99.84	99.71	100.13	100.13	100.00	100.09
15	100.17	99.60	100.27	100.01	100.00	100.27	100.00	100.09
18	100.17	99.60	99.84	99.87	100.00	100.13	100.00	100.04
21	99.83	99.60	100.58	100.00	100.13	99.89	99.87	99.96
24	99.69	99.60	100.58	99.96	100.29	99.89	100.00	100.06
27	99.69	99.86	100.43	99.99	100.00	100.13	100.00	100.04
30	100.00	100.14	100.00	100.05	100.00	100.00	100.00	100.00
35	100.17	100.38	100.27	100.27	100.00	100.00	100.00	100.00
40	100.17	100.26	100.13	100.19	100.20	100.13	100.00	100.14
45	100.00	100.00	99.84	99.95	100.13	100.13	100.00	100.09
50	100.17	100.00	99.41	99.86	100.13	100.13	99.87	100.04
55	100.17	100.00	98.80	99.66	100.00	100.13	99.87	100.00
60	100.00	100.14	98.80	99.65	100.13	100.00	99.87	100.00
70	100.00	100.26	99.09	99.78	100.00	99.89	100.15	100.01
80	100.00	100.52	98.67	99.73	100.00	99.89	99.87	99.92
90	100.17	99.60	98.67	99.48	100.00	100.00	99.72	99.91
100	100.17	99.33	98.51	99.33	100.00	100.00	100.00	100.00
110	100.17	99.60	98.51	99.43	100.00	100.00	99.87	99.96
120	100.17	100.14	98.67	99.66	100.00	100.00	99.60	99.87
100 Per Cent Fringe Order								
	3.54	4.20	3.76		3.81	4.48	3.99	

TABLE 6
Optical Creep, Beam, Concentrated Load, Constant Load
Specimens B-10, B-11, B-12

Time After Loading (min.)	Fringe Reading as Per Cent							
	Tensile Field				Compressive Field			
	B-10	B-11	B-12	Average	B-10	B-11	B-12	Average
0	90.33	90.85	90.86	90.68	87.16	89.45	86.57	87.73
3	92.32	96.40	92.96	93.90	93.01	95.79	92.30	93.70
6	93.54	97.59	94.49	95.21	94.16	97.73	95.32	95.74
9	94.98	98.31	97.24	96.84	95.84	98.41	96.98	97.08
12	97.21	99.28	98.91	98.47	97.51	99.10	98.13	98.25
15	98.64	98.79	99.13	98.85	98.57	99.20	98.13	98.63
18	99.52	98.98	99.78	99.43	99.28	99.78	99.06	99.37
21	99.52	99.39	100.00	99.64	98.98	99.88	99.79	99.55
24	99.86	99.76	100.00	99.87	99.40	99.88	100.00	99.76
27	99.86	100.00	99.78	99.88	99.81	99.88	99.89	99.86
30	100.30	100.00	100.00	100.10	100.43	100.00	99.89	100.11
35	100.08	100.22	99.90	100.06	100.23	100.45	100.09	100.26
40	99.98	100.71	99.90	100.20	100.23	100.45	100.09	100.26
45	100.20	100.98	100.00	100.39	99.92	100.67	100.09	100.23
50	100.42	100.98	100.00	100.47	100.11	100.67	100.00	100.26
55	100.42	100.61	100.34	100.46	100.23	100.90	100.00	100.38
60	100.42	100.71	101.01	100.71	100.43	101.37	100.00	100.60
70	100.86	101.45	100.67	100.99	100.23	101.37	101.14	100.91
80	100.20	102.28	100.24	100.91	100.55	101.47	100.94	100.99
90	100.20	102.01	101.01	101.07	100.87	101.24	100.94	101.02
100	100.76	102.41	101.55	101.57	100.64	102.27	101.35	101.42
110	101.20	102.17	101.01	101.46	100.96	102.71	101.24	101.64
120	101.20	102.54	101.01	101.58	101.49	102.27	101.46	101.74
100 Per Cent Fringe Order								
	5.02	4.61	5.04		5.31	4.90	5.34	

TABLE 7
Optical Creep, Tensile Bar, Constant Load
Specimens C-1, C-3, C-4

Time After Loading (min.)	Fringe Reading as Per Cent				Average
	C-1	C-3	C-4		
0	92.37	87.67	85.69		88.58
3	95.46	97.90	91.92		95.09
6	97.65	99.18	95.46		97.43
9	97.94	99.50	96.13		97.87
12	98.23	100.00	97.13		98.45
15	98.55	99.68	97.28		98.50
18	98.97	99.68	97.64		98.76
21	99.37	99.68	98.64		99.23
24	99.55	99.68	99.15		99.46
27	99.71	99.50	100.00		99.74
30	100.00	100.00	100.00		100.00
35	100.13	100.32	100.82		100.42
40	100.87	100.32	101.15		100.78
45	101.03	100.32	101.99		101.11
50	101.32	100.67	101.99		101.34
55	101.32	101.32	101.99		101.54
60	101.45	101.96	102.51		101.97
70	101.03	102.28	102.84		102.05
80	100.87	102.13	103.36		102.12
90	101.45	102.43	102.18		102.02
100	101.90	101.46	102.18		101.84
110	102.35	101.46	102.51		102.11
120	102.35	101.46	103.51		102.44
100 Per Cent Fringe Order					
	3.79	3.42	3.31		

TABLE 8
Optical Creep, Tensile Bar, Dynamometer Load
Specimens C-5, C-6, C-7

Time After Loading (min.)	<u>Fringe Reading as Per Cent</u>			
	C-5	C-6	C-7	Average
0	90.47	88.52	90.72	89.90
3	99.83	96.72	93.21	96.59
6	99.23	98.20	94.91	97.45
9	99.54	99.85	96.21	98.53
12	99.54	99.17	98.70	99.14
15	100.00	99.35	98.77	99.37
18	99.84	99.50	99.34	99.56
21	99.84	100.00	99.76	99.87
24	99.84	99.82	100.00	99.89
27	99.84	100.00	100.00	99.95
30	100.14	100.00	100.00	100.05
35	100.14	100.32	100.00	100.15
40	100.43	100.65	99.48	100.19
45	100.43	100.97	99.88	100.43
50	100.43	100.97	100.00	100.47
55	100.00	100.97	100.28	100.42
60	100.27	101.45	100.00	100.57
70	100.60	101.80	100.14	100.85
80	100.60	101.95	100.52	101.02
90	100.60	102.12	100.80	101.17
100	100.87	102.12	100.80	101.26
110	100.60	101.95	101.46	101.34
120	100.87	101.95	101.46	101.43
100 Per. Cent Fringe Order				
	3.68	3.39	4.24	

TABLE 9
Optical Creep, Tensile Bar, Constant Strain
Specimens C-8, C-9, C-10

Time After Loading (min.)	<u>Fringe Reading as Per Cent</u>			
	C-8	C-9	C-10	Average
0	93.04	89.11	92.29	91.48
3	98.08	92.94	99.51	96.84
6	98.96	96.04	99.51	98.17
9	99.25	98.09	99.69	99.01
12	100.00	98.54	100.18	99.57
15	100.29	98.99	100.37	99.88
18	100.75	99.58	99.69	100.01
21	100.75	99.73	100.18	100.22
24	100.75	99.87	99.85	100.16
27	100.29	100.00	99.85	100.04
30	100.29	100.00	100.00	100.07
35	99.25	100.00	100.00	99.75
40	99.25	100.00	99.69	99.65
45	99.84	100.00	100.00	99.94
50	99.71	100.48	99.69	99.96
55	99.09	100.32	100.68	100.03
60	99.57	100.32	100.18	100.02
70	100.16	100.48	100.18	100.27
80	101.09	100.61	101.39	101.03
90	100.91	100.48	101.54	100.98
100	101.04	102.23	102.06	101.77
110	101.33	102.68	101.39	101.80
120	100.75	102.97	102.06	101.93
100 Per Cent Fringe Order				
	3.75	3.77	3.24	

TABLE 10
Optical Creep Curved Beam, Constant Strain
Specimens D-1, D-2, D-3

Time After Loading (min.)	Fringe Reading as Per Cent							
	Tension Field				Compressive Field			
	D-1	D-2	D-3	Average	D-1	D-2	D-3	Average
0	106.63	101.32	99.57	102.51	103.57	94.66	98.74	98.99
3	102.61	96.66	98.59	99.29	101.61	92.65	97.90	97.39
6	102.61	98.54	98.72	99.96	100.80	95.10	95.77	97.22
9	101.41	98.54	98.87	99.61	103.21	99.56	95.35	99.37
12	101.63	99.18	99.16	99.99	103.01	99.12	96.00	99.37
15	101.19	99.45	99.44	100.03	103.21	100.44	97.44	100.36
18	100.40	99.59	99.85	99.95	102.71	100.00	98.51	100.41
21	100.62	99.18	99.72	99.84	101.36	99.76	99.58	100.23
24	100.40	99.59	100.00	100.00	100.50	99.32	100.23	100.02
27	100.00	99.74	100.00	99.91	99.40	100.00	99.81	99.74
30	100.40	100.00	100.15	100.22	99.65	100.00	100.23	99.96
35	99.61	100.12	100.00	99.91	100.50	100.00	99.81	100.10
40	100.40	100.65	99.57	100.21	100.50	99.59	99.58	99.89
45	100.18	101.06	99.44	100.23	100.50	100.00	99.58	100.03
50	100.40	101.32	99.28	100.33	101.06	100.44	99.39	100.30
55	100.62	100.00	99.29	99.97	100.80	100.44	99.39	100.21
60	100.62	99.45	99.57	99.88	100.50	100.00	98.97	99.82
70	100.40	99.59	99.57	99.85	100.50	100.00	99.16	99.89
80	100.18	100.00	99.44	99.87	100.50	100.00	99.58	100.03
90	100.18	99.74	99.28	99.73	100.50	97.31	98.51	98.77
100	101.01	98.54	99.16	99.57	99.95	97.95	97.90	98.60
110	100.18	99.06	99.44	99.56	100.50	97.55	98.51	98.85
120	100.40	98.80	99.44	99.54	101.06	96.42	97.71	98.40
100 Per Cent Fringe Value								
	2.76	4.17	3.91		1.99	2.49	2.62	

TABLE 11
Optical Creep Curved Beam, Dynamometer Load
Specimens D-4, D-5, D-6

Time After Loading (min.)	Fringe Reading as Per Cent							
	Tension Field				Compressive Field			
	D-4	D-5	D-6	Average	D-4	D-5	D-6	Average
0	99.56	99.35	98.71	99.21	99.70	99.04	91.06	96.60
3	99.72	98.12	99.28	99.04	100.84	97.71	91.74	96.76
6	99.85	98.88	99.41	99.38	100.23	99.04	93.07	97.45
9	99.72	99.13	99.41	99.42	98.32	99.41	95.57	97.77
12	100.13	99.62	99.84	99.86	98.74	99.21	96.86	98.27
15	100.13	99.51	99.84	99.83	100.00	100.75	98.47	99.74
18	100.00	100.00	100.00	100.00	98.97	100.06	100.68	100.20
21	100.28	99.51	100.13	99.97	98.97	100.55	100.68	100.06
24	99.85	99.87	100.13	99.95	99.58	100.17	100.48	100.08
27	100.13	99.87	99.72	99.91	100.65	99.62	100.48	100.25
30	100.00	100.00	99.84	99.95	100.00	100.00	100.00	100.00
35	100.00	100.36	100.13	100.16	100.00	99.80	99.80	99.87
40	100.13	99.87	100.00	100.00	99.58	99.21	99.11	99.30
45	99.72	99.87	100.00	99.86	100.00	99.04	97.34	98.79
50	99.85	99.87	100.00	99.91	99.58	99.41	97.34	98.78
55	100.00	99.51	100.28	99.93	98.97	99.41	97.78	98.72
60	100.13	99.35	100.13	99.87	99.16	99.80	97.78	98.91
70	100.41	99.62	99.84	99.96	99.16	100.17	98.47	99.26
80	100.13	99.24	100.13	99.83	99.58	100.17	97.99	99.25
90	100.13	98.99	100.00	99.71	98.97	99.80	97.78	98.85
100	100.28	99.51	100.57	100.12	98.32	99.41	97.99	98.57
110	100.00	99.24	100.00	99.75	98.74	99.62	98.47	98.94
120	100.13	98.88	100.00	99.67	99.16	99.21	98.47	98.95
100 Per Cent Fringe Value								
	3.88	4.47	3.87		2.62	2.93	2.48	

TABLE 12
Optical Creep, Curved Beam, Constant Load
Specimens D-7, D-8, D-9

Time After Loading (min.)	Fringe Reading as Per Cent							
	Tension Field				Compressive Field			
	D-7	D-8	D-9	Average	D-7	D-8	D-9	Average
0	90.38	88.01	92.03	90.14	92.72	75.60	91.29	86.54
3	95.42	95.31	97.43	96.05	92.88	94.42	94.67	93.99
6	98.06	95.19	97.43	96.89	96.16	96.69	94.67	95.84
9	98.39	96.36	98.79	97.85	98.92	97.51	95.58	97.34
12	98.76	96.88	98.64	98.09	99.28	98.14	96.65	98.02
15	99.55	97.79	98.79	98.71	99.28	98.14	97.55	98.32
18	99.55	97.89	99.47	98.97	100.20	98.55	98.56	99.07
21	99.67	98.57	100.53	99.59	99.80	99.18	100.00	99.66
24	99.32	99.08	100.12	99.51	100.00	99.59	100.00	99.86
27	99.90	99.60	100.12	99.87	100.00	100.00	100.00	100.00
30	100.00	100.00	100.00	100.00	99.80	100.00	99.39	99.73
35	100.25	100.12	100.12	100.16	100.00	100.18	100.13	100.10
40	100.70	100.54	99.85	100.36	100.36	100.18	100.00	100.18
45	100.58	100.92	100.66	100.72	100.56	100.41	100.00	100.32
50	101.23	100.92	102.40	101.52	100.92	100.18	100.60	100.57
55	101.73	101.29	102.55	101.86	101.08	100.00	100.00	100.36
60	102.64	101.43	102.84	102.30	101.64	100.00	99.84	100.49
70	102.24	102.23	103.91	102.79	102.00	100.00	101.07	101.02
80	102.77	102.23	104.17	103.06	102.00	100.82	100.77	101.20
90	102.42	101.95	104.17	102.84	102.36	100.00	100.77	101.04
100	102.99	101.17	104.59	102.92	102.36	100.82	101.37	101.52
110	102.22	101.83	104.06	103.04	102.92	100.82	101.37	101.70
120	104.38	101.69	105.25	103.77	102.92	100.18	102.28	101.79
100 Per Cent Fringe Value								
	4.84	4.26	4.12		3.05	2.69	3.64	

TABLE 13

Optical Creep, Disk in Compression, Constant Load
Specimens E-1, E-2, E-3

Time After Loading (min.)	<u>Fringe Reading as Per Cent</u>			
	E-1	E-2	E-3	Average
0	101.69	97.44	100.97	100.03
3	101.69	99.22	102.95	101.29
6	100.00	98.99	102.46	100.48
9	98.01	98.72	99.74	98.88
12	97.13	98.22	98.55	97.97
15	96.83	98.22	97.80	97.62
18	97.13	98.72	99.03	98.29
21	98.01	98.49	98.77	98.42
24	98.57	99.73	99.30	99.20
27	98.82	99.50	99.30	99.21
30	100.00	100.00	100.00	100.00
35	100.26	100.23	100.97	100.49
40	101.38	100.50	101.94	101.27
45	102.25	100.78	101.50	101.51
50	101.94	101.00	101.23	101.39
55	101.94	100.23	100.00	100.72
60	101.69	100.78	100.26	100.91
70	101.38	101.00	100.00	100.79
80	101.69	102.28	100.97	101.65
90	101.94	102.28	100.97	101.73
100	101.94	101.51	100.97	101.47
110	101.69	101.51	100.53	101.24
120	101.69	102.51	100.97	101.72
100 Per Cent of Fringe Order				
	1.96	2.19	2.27	

TABLE 14
Optical Creep Disk in Compression, Dynamometer Load
Specimens E-4, E-5, E-6

Time After Loading (min.)	Fringe Reading as Per Cent			
	E-4	E-5	E-6	Average
0	102.85	99.46	95.81	99.37
3	103.16	101.27	96.91	100.45
6	103.16	100.00	96.91	100.02
9	101.14	98.96	97.21	99.10
12	100.25	98.23	97.76	98.75
15	99.68	98.46	98.06	98.73
18	100.00	98.96	97.76	98.91
21	100.00	98.96	98.85	99.27
24	99.68	99.23	99.70	99.54
27	99.68	99.23	99.15	99.35
30	100.00	99.55	100.25	99.93
35	99.68	100.45	100.80	100.31
40	101.14	101.72	101.10	101.32
45	103.16	100.45	101.35	101.65
50	102.02	100.73	100.25	101.00
55	102.02	100.73	99.70	100.82
60	102.02	100.73	100.25	101.00
70	101.71	101.27	100.80	101.26
80	102.59	101.72	101.65	101.99
90	103.16	101.72	101.65	102.18
100	102.85	101.27	101.89	102.00
110	101.45	100.45	101.89	101.26
120	102.28	101.99	101.89	102.05
100 Per Cent Fringe Value				
	1.928	2.21	2.01	

TABLE 15
Optical Creep, Disk in Compression, Constant Strain
Specimens E-7, E-8, E-9

Time After Loading (min.)	Fringe Reading as Per Cent			
	E-7	E-8	E-9	Average
0	104.85	102.87	108.68	105.47
3	102.01	102.87	106.97	103.95
6	98.56	100.28	101.15	100.00
9	98.56	99.48	99.75	99.26
12	99.43	99.48	97.79	98.90
15	100.26	99.25	98.09	99.20
18	100.00	99.48	98.65	99.38
21	99.69	99.48	98.90	99.36
24	100.00	99.48	98.90	99.46
27	99.69	99.48	100.30	99.82
30	100.00	100.00	99.20	99.73
35	99.43	100.80	100.85	100.36
40	100.00	101.60	100.30	100.63
45	99.43	101.04	100.30	100.26
50	100.00	100.52	98.90	99.81
55	100.26	100.52	98.90	99.89
60	101.13	100.00	98.90	100.01
70	100.88	100.80	99.45	100.38
80	99.69	100.80	99.75	100.08
90	100.00	101.32	99.45	100.26
100	101.44	100.52	99.75	100.57
110	100.57	100.52	99.75	100.28
120	100.26	101.04	100.30	100.53
100 Per Cent Fringe Value				
	1.94	2.12	1.99	

BIBLIOGRAPHY

1. Coker, E. G., and L. N. G. Filon, A Treatise on Photoelasticity. Cambridge: Cambridge University Press, 1931.
2. Norris, Charles H., "Model Analysis of Structures," Proceedings of the Society for Experimental Stress Analysis, Vol. 1, No. 2, July 1944, pp. 18 - 34.
3. Zener, Clarence, Elasticity and Anelasticity of Metals. Chicago: University of Chicago Press, 1948.
4. Heywood, R. B., Designing by Photoelasticity. London, Chapman and Hall Limited, 1952.